medRxiv preprint doi: https://doi.org/10.1101/2021.01.22.21250282; this version posted February 6, 2021. The copyright holder for this preprint (which was not certified by peer review) is the author/funder, who has granted medRxiv a license to display the preprint in perpetuity. It is made available under a CC-BY 4.0 International license .

Model-driven mitigation measures for reopening schools during the COVID-19 pandemic.

Ryan S. McGee[*,1,a], Julian R. Homburger[*,2,b], Hannah E. Williams[2,c], Carl T. Bergstrom[†,1,d], and Alicia Y. Zhou[†,2,e]

[*]Co-first authors; corresponding authors. [†]Co-senior authors.
[1]Department of Biology, University of Washington, Seattle WA 98195
[2]Color Health, Burlingame, CA

Email: [a]ryansmcgee@gmail.com, [b]jrh@color.com, [c]hannah@color.com, [d]cbergst@uw.edu, [e]alicia@color.com

Abstract: Reopening schools is an urgent priority as the COVID-19 pandemic drags on. To explore the risks associated with returning to in-person learning and the value of mitigation measures, we developed stochastic, network-based models of SARS-CoV-2 transmission in primary and secondary schools. We find that a number of mitigation measures, alone or in concert, may reduce risk to acceptable levels particularly when community prevalence is low. Student cohorting, in which students are divided into two separate populations that attend in-person classes on alternating schedules, can reduce both the likelihood and the size of outbreaks. Proactive testing of teachers and staff once or twice a week can help catch introductions early, before they spread widely through the school. In secondary schools, where the students are more susceptible to infection and have different patterns of social interaction, control is more difficult. Especially in these settings, planners should also consider testing students once or twice weekly. Vaccinating teachers and staff protects these individuals and—when vaccines block SARS-CoV-2 transmission in addition to symptoms—may also have a protective effect on students as well. Other mitigations, including mask-wearing, social distancing, and increased ventilation, remain a crucial component of any reopening plan.

NOTE: This preprint reports new research that has not been certified by peer review and should not be used to guide clinical practice.

medRxiv preprint doi: https://doi.org/10.1101/2021.01.22.21250282; this version posted February 6, 2021. The copyright holder for this preprint (which was not certified by peer review) is the author/funder, who has granted medRxiv a license to display the preprint in perpetuity. It is made available under a CC-BY 4.0 International license .

Introduction

As the COVID-19 pandemic accelerated in early 2020, schools across the world closed in an effort to preempt school-associated transmission and protect their students, teachers, and staff. By mid-April of that year, 195 countries had closed their schools in response to COVID-19, affecting more than 1.5 billion students (1). In the United States (US), schools were among the first organizations to close, and many remained closed or transitioned to remote learning through the end of the 2019-20 school year. Many remain closed today. While remote learning affords students the opportunity to continue their education, it fails to provide many of the crucial benefits students typically receive through in-person schooling (2). There is an urgent need to evaluate the effectiveness of evidence-based strategies that would allow children, teachers, and staff to safely return to in-person learning.

To date, widespread community transmission, conflicting public health guidance, and the emergence of new SARS-CoV-2 variants associated with higher transmissibility have compounded the challenges schools face when reopening (3–5). Numerous epidemiological models have been developed to forecast the spread of SARS-CoV-2 or compare the effectiveness of mitigation strategies in communities or large populations (6–12). However, only a few models have focused on the unique demographic and contact structures of primary and secondary school settings (13–15).

Case studies suggest that primary schools have a lower risk of transmission compared to secondary schools (16–19). Two principal causes are likely at play. First, younger children are less likely than adolescents or adults to become infected with SARS-CoV-2 (20), and less likely to experience symptomatic or severe disease (21, 22). Second, primary and secondary schools have different contact structures. Primary school students have fewer contacts and typically spend the full day with a single teacher and the same group of students. By contrast, secondary school students move between classrooms and encounter multiple teachers and groups of students each day.

We have developed epidemiological models to simulate the spread of SARS-CoV-2 amongst students, teachers, and staff in both primary and secondary schools. Here, we use these models to better understand the risks of reopening schools and to explore the effectiveness of different mitigation strategies: cohorting students, proactive testing, quarantine protocols, and vaccinating teachers and staff.

Model and methods

A stochastic network-based model of SARS-CoV-2 transmission

We use the SEIRS+ modeling framework (https://github.com/ryansmcgee/seirsplus) to study the dynamics of disease transmission in school populations. SEIRS+ builds upon classic SEIR compartment models that divide the population into susceptible (S), exposed (E), infectious (I), and recovered (R) individuals (23) and track the transitions of individuals among these states. The basic SEIR model is a deterministic model of a homogeneous population with well-mixed contacts. However, accounting for demographic heterogeneity and the structure of contact networks (24, 25) is particularly important when evaluating control strategies that perturb the contact network (e.g., social distancing) or making use of it (e.g., contact tracing). For disease control, modeling stochasticity is crucial to understand the distribution of potential outcomes, especially in smaller populations.

To incorporate these important aspects of disease dynamics, we use the SEIRS+ modeling framework to implement an extended SEIR model of SARS-CoV-2 transmission on stochastic dynamical networks. Individuals

medRxiv preprint doi: https://doi.org/10.1101/2021.01.22.21250282; this version posted February 6, 2021. The copyright holder for this preprint (which was not certified by peer review) is the author/funder, who has granted medRxiv a license to display the preprint in perpetuity. It is made available under a CC-BY 4.0 International license .

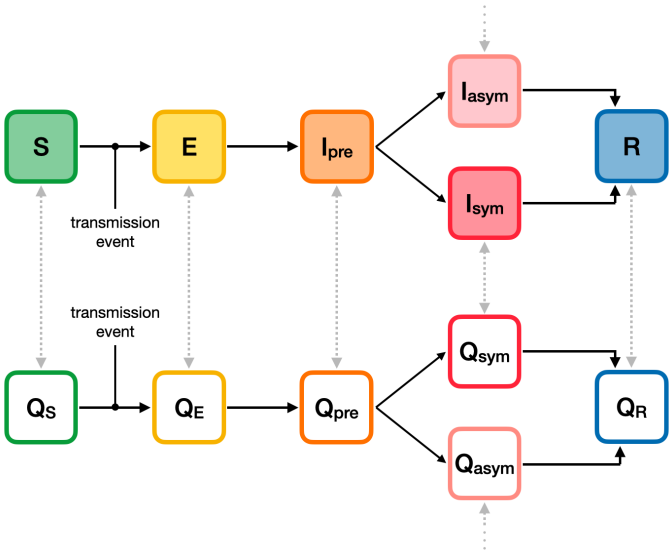

Figure 1: Compartment model. The progression of disease states in the Extended SEIR Network Model is represented by the compartments shown. Susceptible (S) individuals become infected (exposed) following transmissive contact with an infectious individual. Newly exposed (E) individuals undergo a latent period, during which time they are infected but not contagious. Infected individuals then progress to a pre-symptomatic infectious state (I_{pre}), in which they are contagious but not yet presenting symptoms. Some infectious individuals go on to develop symptoms (I_{sym}); while others will remain asymptomatic (I_{asym}). At the conclusion of the infectious period, infected individuals enter the recovered state (R) and are no longer contagious or susceptible to infection. The unshaded compartments represent quarantined individuals in the respective disease states.

are represented as nodes in a contact network. Parameters, interactions, interventions, and residence times in each compartment are specified on an individual-by-individual basis. This allows us to model realistic heterogeneities in disease, transmission, and behavioral parameters—which are particularly important when considering SARS-CoV-2 transmission dynamics in small, age-stratified school populations. The disease dynamics are summarized in Figure 1 and described in detail in Appendix A.1. Parameter settings are listed in Appendix A.2.1.

We model infection as transmitted largely along a network of close contacts. Close contacts are individuals with whom one has repeated, sustained, or close-proximity interactions on a regular basis: classmates, friends, housemates, or other close relationships. Disease transmission can also occur among casual contacts—individuals who are not on one's contact network, but with whom one has incidental, brief, or superficial interactions. A network locality parameter sets the relative frequency and weight of transmission among close and casual contacts (Appendix A.1.4). In both primary and secondary school settings, we assume that 80% of transmission occurs between close contacts specified by the networks. Exposure to the community is modeled by randomly introducing new cases to the school population at a rate that corresponds to the community prevalence—see the Community prevalence and case introduction rate section below.

The likelihood that a given susceptible individual becomes infected depends on the prevalence of infectious individuals among their contacts, the transmissibilities of these contacts, and their own susceptibility to infection (Appendix A.1.4). We assume an over-dispersed distribution of individual variation in transmissibility (Appendix A.2.2), which corresponds to the observation that 80% of SARS-CoV-2 transmission may be attributable to 20% of infectious individuals (26, 27). This distribution of individual transmissibilities is calibrated to a nominal basic reproduction number (R_0) for the population. While the R_0 of SARS-CoV-2 varies, many estimates land

medRxiv preprint doi: https://doi.org/10.1101/2021.01.22.21250282; this version posted February 6, 2021. The copyright holder for this preprint (which was not certified by peer review) is the author/funder, who has granted medRxiv a license to display the preprint in perpetuity. It is made available under a CC-BY 4.0 International license .

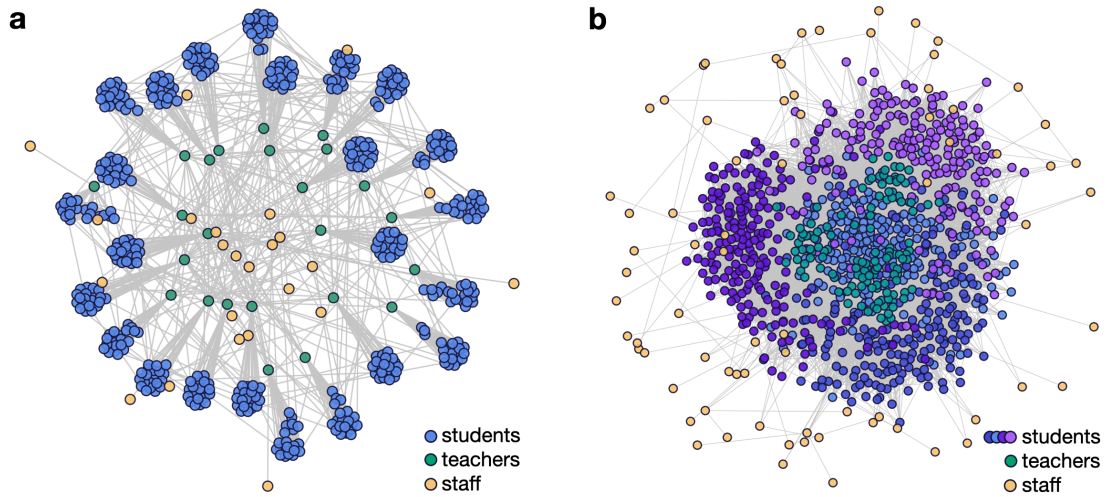

Figure 2: Network structures for primary and secondary schools. Each individual is represented by a circle, with grey lines connecting close contacts. (**a**) Primary school students (blue) are organized into classes with close contacts between all students in each classroom as well as a single teacher (green). School staff (yellow) interact with teachers and other staff. (**b**) Secondary school students (shades of blue and purple indicating grade levels) move between classrooms and have close contact with six teachers (green) each. School staff (yellow) interact with teachers and other staff. Secondary school students are clustered into loose social groups and are more likely to interact with other students in the same grade.

in the vicinity of 2.5-3.0 without intervention (28–32). As a baseline, we assume that schools will implement sufficient mitigation measures, such as mask wearing, physical distancing, and heightened hygiene, to reduce R_0 to 1.5 in the school population. More aggressive mitigation measures may bring the baseline R_0 in schools closer to 1.0; results for other values of R_0 are provided in the Supporting Figures.

Individuals in any disease state may enter quarantine due to symptoms or in response to a positive test result. The effect of isolating individuals is modeled by introducing compartments that represent quarantined individuals who do not make transmissive contact with others outside of the home (Figure 1, Appendix A.2.3.3). Individuals remain in quarantine for 10 days (33), at which time they transition to the non-quarantine compartment corresponding to their present disease state. We assume that 20% of symptomatic individuals self-isolate upon the onset of symptoms.

Model considerations for primary schools versus secondary schools

We use distinct models for primary and secondary schools, with different contact networks reflecting the social structures in each setting (Appendix A.2). We assume primary school children are 60% as susceptible as adults, while secondary school students are equally susceptible to adults. Our primary school model encompasses a school with 480 students, 24 teachers, and 24 additional staff. Primary school students have close contacts with their teacher, classmates, and other children in their household (e.g., siblings). For our secondary school model, we simulate a school with 800 students distributed across four grades, 125 teachers, and 75 additional staff. Secondary school students have close contacts with six teachers, with other students in their grade and social groups, and with other students in their households. Both settings feature a network of close contacts among teachers and staff. A new random network is generated for each simulation replicate. Example network diagrams for each school setting are shown in Figure 2. Detailed descriptions of the contact network structures and their generation are provided in Appendix A.2.3.

medRxiv preprint doi: https://doi.org/10.1101/2021.01.22.21250282; this version posted February 6, 2021. The copyright holder for this preprint (which was not certified by peer review) is the author/funder, who has granted medRxiv a license to display the preprint in perpetuity. It is made available under a CC-BY 4.0 International license .

Community prevalence and case introduction rate

To account for the effect of community prevalence on COVID-19 dynamics in schools, we model scenarios in which new cases are introduced into the school population stochastically at rates corresponding to daily, weekly, or monthly introductions on average (Appendix A.2.4). When the effective community reproduction number R_{eff} is in the 1.0–2.0 range, these rates approximately correspond to the community prevalences shown in Table Table A.2.4. We also consider the consequences of a single introduction; in this scenario, all replicates start off with the case introduction occurring on the first day of the simulation.

Simulations

To capture stochastic variability in outcomes, we report 1,000 replicates for each parameter set. Each replicate simulation tracks the progression of an outbreak that begins with the introduction of a single infected individual in an otherwise disease-free school population. The simulation begins on a random day of the week with the introduction of an initial case. Additional introductions may occur throughout the simulation at a Poisson rate reflecting the community prevalence. School is in session 5 days a week, and we assume that no close contacts are made outside of the household on weekends. Weekend transmission among casual contacts does occur. The simulation proceeds for 150 days to represent a school semester.

To allows comparisons across scenarios with different community prevalences, we report the percentage of cases attributable to transmissions within the school population (i.e., excluding introduced cases attributable to exogenous community exposure). These transmissions may occur either at school or among school-affiliated individuals while off campus, and are hereafter collectively described as "school transmission". We define "sizable outbreaks", as simulation runs where more than 5% of the population becomes infected in school over the course of the semester (150 days). While schools that experience sizable outbreaks are likely to stop in-person learning before very large case counts are realized, these data provide information about the probability of epidemic trajectories that could require such action.

Results

The effect of community prevalence

The prevalence of COVID-19 in the community impacts the risk of transmission in schools. Figure 3 shows the percentage of the school population infected in primary and secondary schools over the course of a semester when only basic mitigation strategies (e.g. distancing, hygiene, and mask wearing) are in place. Higher COVID-19 prevalence in the surrounding community increases the probability of a sizable outbreak in primary and secondary schools alike. When community prevalence is so high that new introductions occur on a daily basis (between 0.25–1.0%), our simulations suggest that even aggressive mitigation strategies cannot prevent sizable outbreaks (Figure 5).

The probabilities of sizable outbreaks are higher in secondary schools than in primary schools, and the outbreaks tend to be larger in secondary schools. This difference generally holds across the range of parameters and interventions that we explore, and presumably arises because secondary school students are more susceptible and have more interconnected contact networks.

medRxiv preprint doi: https://doi.org/10.1101/2021.01.22.21250282; this version posted February 6, 2021. The copyright holder for this preprint (which was not certified by peer review) is the author/funder, who has granted medRxiv a license to display the preprint in perpetuity. It is made available under a CC-BY 4.0 International license .

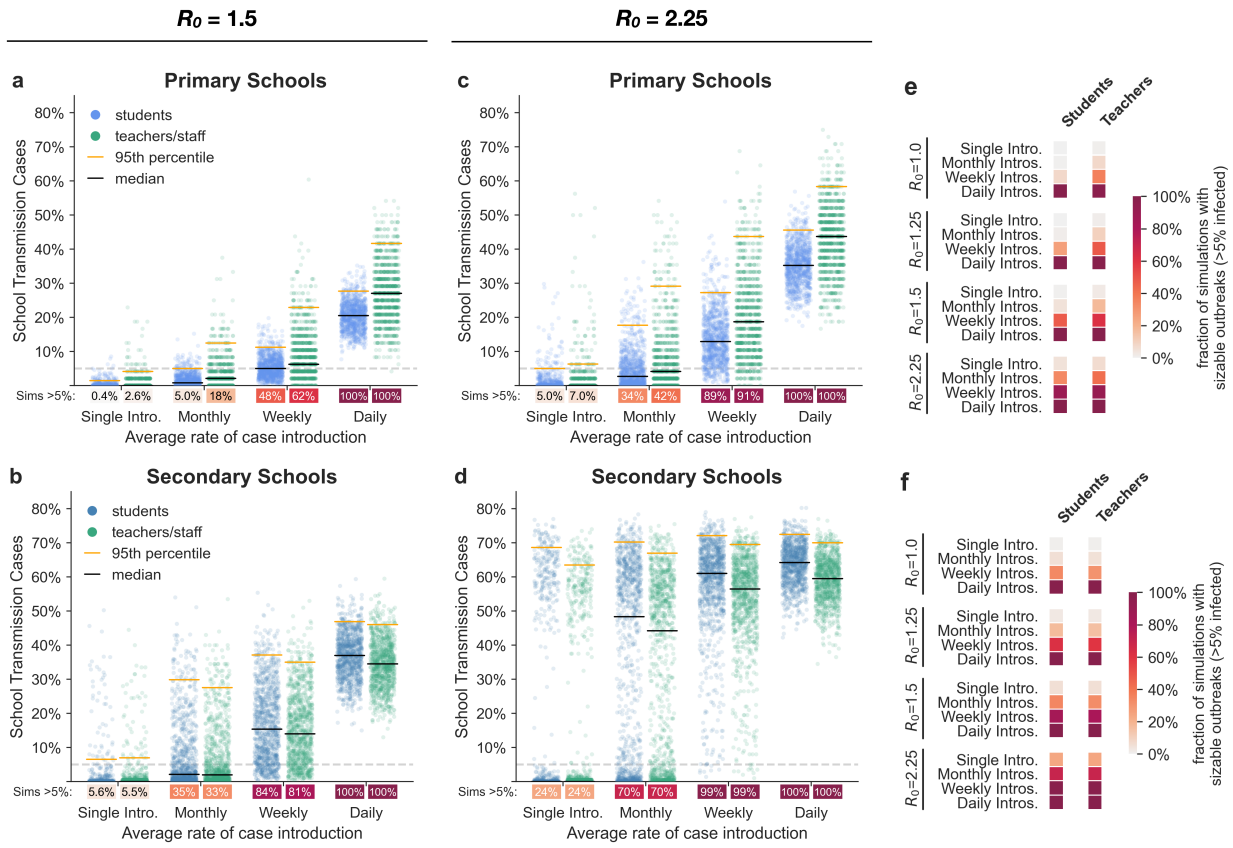

Figure 3: Effect of community prevalence. The distributions of school transmission cases as a percentage of the school population when new cases are introduced at different average rates. In these simulations, all students are in school five days a week and there is no proactive testing. (**a,b**) Outcomes for primary schools and secondary schools, respectively, with baseline transmission R_0=1.5. Black and orange lines represent median and 95th percentile outcomes, respectively. Under each jitter distribution we list the percentage of simulations where more than 5% (grey dashed line) of the population are infected in school. (**c,d**) Outcomes for primary and secondary schools in scenarios with heightened transmission R_0=2.25 due to the predominance of a highly-transmissible strain. (**e,f**) Heatmaps show the fraction of simulations where more than 5% of the student or teacher population are infected in primary and secondary schools, respectively, across a range of R_0 values and introduction rates.

The effect of highly-transmissive variants

As of February 2021, several SARS-CoV-2 variants appear to have evolved higher transmissibility relative to their ancestors (3). For example, the B.1.1.7 lineage that has spread throughout the UK appears to be 30%-70% more transmissible than previous SARS-CoV-2 variants (3, 34, 35). To understand how highly transmissible variants might impact transmission dynamics should they become predominent, we look at the consequences of a 50% increase in transmissibility, which increases the assumed baseline R_0 for the school environment from R_0=1.5 to R_0=2.25. Results for more incremental increases in mean transmission rates that approximate intermediate penetrance of such strains can be found in the Supporting Figures.

Figure 3 illustrates how community prevalence, as modeled by introduction rate, influences school transmissions when schools are confronted by this more transmissible strain. Even under a monthly rate of new case introductions, schools face the risk of a major outbreak. With more frequent introductions, substantive outbreaks become the most likely outcome. Aggressive controls mitigate the risk somewhat, but are considerably less effec-

medRxiv preprint doi: https://doi.org/10.1101/2021.01.22.21250282; this version posted February 6, 2021. The copyright holder for this preprint (which was not certified by peer review) is the author/funder, who has granted medRxiv a license to display the preprint in perpetuity. It is made available under a CC-BY 4.0 International license .

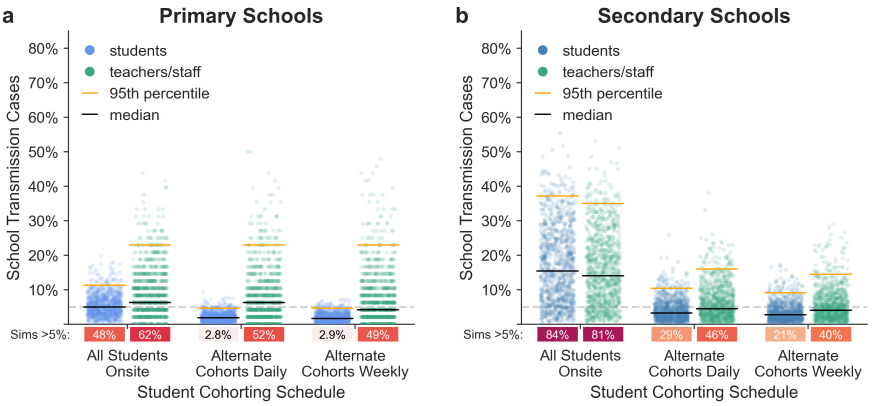

Figure 4: Effects of cohorting strategies. The distributions of school transmission cases as a percentage of school population for 1,000 simulations under different student cohorting strategies in (**a**) primary schools and (**b**) secondary schools with R_0=1.5, approximately weekly new case introductions, and all students on campus five days a week. Under each jitter distribution we list the percentage of simulations that result in outbreaks affecting more than 5% of the population.

tive for a strain with R_0=2.25 than for a strain with R_0=1.5 (Figure 5).

The effects of interventions

Cohorting

Cohorting, wherein students are divided into two or more groups that alternate in-person learning, is a common strategy for mitigating outbreak in school settings (36–38). In our model, we represent cohorting by shifting the contact networks according to which students are on campus (Appendix A.2.3.5). While off campus, students are disconnected from the school network but maintain household connections and transmission to casual contacts (the latter representing out-of-school interactions among the student body). Teachers remain on campus across all cohorts.

Figure 4 shows the effects of three common cohorting strategies: (1) all students belong to a single cohort that is on campus full time, (2) students are divided into two cohorts, A and B, which are on campus on alternating days, and (3) students are divided into two cohorts which are on campus on alternating weeks (Appendix A.2.5.3). We find that relative to no cohorting, alternating day and alternating week strategies can improve outcomes substantially. Cohorting with alternating weeks outperforms cohorting with alternating days, particularly in primary schools. In primary schools, student cohorting alone dramatically reduces the risk of outbreak amongst students. In secondary schools, cohorting is helpful but is insufficient on its own to keep the likelihood of an outbreak low amongst students or amongst teachers and staff.

Proactive Testing

The purpose of proactive testing is to identify individuals who are infected but not currently showing symptoms, so that they can be quarantined (39, 40). We consider five proactive testing strategies, detailed in Appendix A.2.5.2: (1) a baseline of no testing, (2) once-weekly testing amongst teachers and staff only, (3) twice-weekly testing amongst teachers and staff only, (4) once-weekly testing cadence amongst students, teachers, and staff, and (5) twice-weekly testing amongst students, teachers, and staff. We assume that 75% of students and 100% of teachers

medRxiv preprint doi: https://doi.org/10.1101/2021.01.22.21250282; this version posted February 6, 2021. The copyright holder for this preprint (which was not certified by peer review) is the author/funder, who has granted medRxiv a license to display the preprint in perpetuity. It is made available under a CC-BY 4.0 International license .

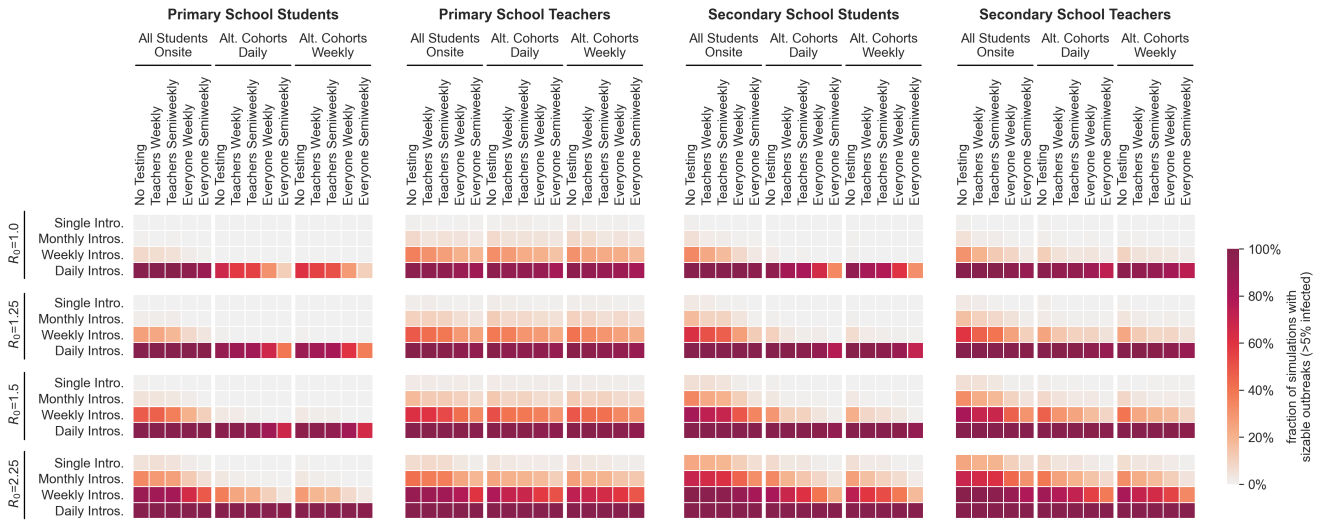

Figure 5: Effects of cohorting and testing strategies. Heatmaps illustrate the interactions of three student cohorting strategies and five proactive testing strategies (horizontal axis) across a range of transmission levels (R_0) and new case introduction rates (vertical axis). The color of each cell indicates the fraction of 1,000 simulations for the given parameter set that result in sizable outbreaks where more than 5% of the population is infected. Outcomes are shown for student and teacher populations in primary and secondary schools as indicated by the title above each heatmap.

and staff are compliant with testing. Previous work suggests that long test turnaround times severely curtail the value of testing. To account for this, we use a test turnaround time of 24 hours and assume positive individuals enter quarantine immediately (39, 41, 42).

Figure 5 illustrates the effects of cohorting and testing on the probability of sizable outbreaks. In our model, proactive testing consistently reduces the risk of outbreaks among teachers and students (Figure 5, Supporting Figures). While cohorting alone does not completely mitigate the risk of sizable outbreaks in secondary schools, the combination of cohorting and testing can keep this risk in check when baseline transmissibility in the school is sufficiently low.

Figure 6 highlights the interactions between testing and cohorting measures in their effect on outbreak size in a secondary school environment. More aggressive testing helps reduce the size of outbreaks, as does more aggressive cohorting. and testing and cohorting together outperform either measure alone. Individual interventions that help students also help teachers, and vice versa. However, specific interventions may help one group more than another. Testing teachers confers greater marginal benefits on teachers than it does on students. Cohorting, by contrast, helps students more than teachers. Teachers remain on campus five days a week whether cohorting is practiced or not, whereas students spend half of their time at home with minimal exposure under a cohorting plan.

Isolation protocols

When an infected individual is identified by proactive testing, that person should be immediately isolated to prevent further transmission. In primary schools where classroom organization is stable, school administrators may additionally consider quarantining the entire classroom—students and teacher—involved.

Our model indicates that classroom-level quarantine can reduce outbreak risk (Figure A4). For students and for teachers, with weekly introductions, the distribution of outcomes from isolating classrooms is significantly

medRxiv preprint doi: https://doi.org/10.1101/2021.01.22.21250282; this version posted February 6, 2021. The copyright holder for this preprint (which was not certified by peer review) is the author/funder, who has granted medRxiv a license to display the preprint in perpetuity. It is made available under a CC-BY 4.0 International license .

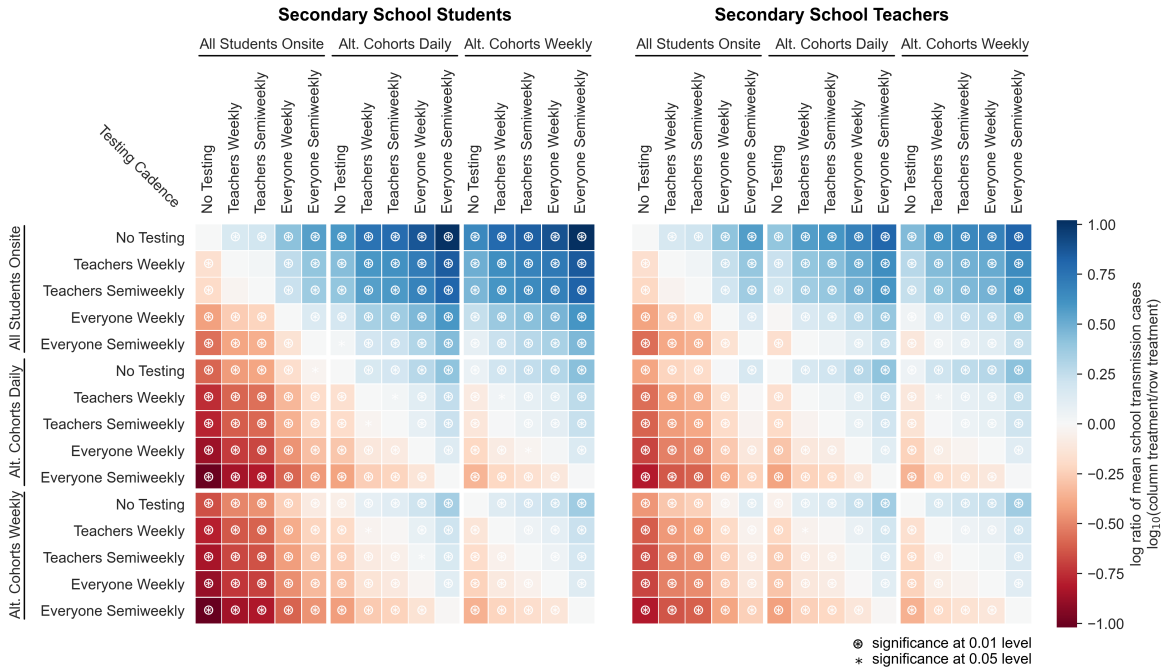

Figure 6: Relative effects of testing and cohorting in a secondary school setting. A heatmap of pairwise comparisons of testing and cohorting interventions illustrates the effects of various combinations on mean outbreak sizes. Results are shown for scenarios where R_0=1.5, case introductions occur weekly on average, and only the positive individual is quarantined when cases are detected. Each cell is colored according to the log-ratio of mean outbreak sizes for the two interventions, which represents the effect of the column intervention relative to the row intervention (i.e., a blue cell indicates that the column intervention achieves a lower mean outbreak size than the row intervention). Symbols in cells denote statistically significant differences in outbreak size distributions according to the Mann-Whitney U test at the 0.01 (⊛) and 0.05 (∗) levels.

more favorable than that from isolating individuals (Mann-Whitney U test, $p \ll 0.01$). When introductions are less frequent, benefits of classroom isolation may not be statistically significant. One important consideration for quarantining at the classroom-level is that this approach imposes more quarantine days on the population. When choosing a quarantine strategy, the costs of in-person learning days lost, both by students and by teachers, should be taken into account.

Vaccination

Pfizer-BioNTech and Moderna have reported extremely encouraging results from their phase III COVID-19 vaccine trials, with 90% or greater efficacy at blocking symptomatic disease (43, 44). Distribution of both vaccines are underway in the US. Other effective vaccines appear to be close behind in the pipeline. In many locales, school teachers and staff are being prioritized for vaccination immediately after high-risk individuals and frontline workers (45).

Because all COVID-19 vaccine trial data to date have focused only on diagnosis of symptomatic disease as a primary endpoint, we do not know the degree to which COVID-19 vaccines block transmission. As such, we consider scenarios in which post-vaccination transmissibility is reduced by 100% and by just 50% in the model (Appendix A.2.5.5).

Teachers and staff who have been vaccinated against COVID-19 with a 90% effective vaccine are well-

medRxiv preprint doi: https://doi.org/10.1101/2021.01.22.21250282; this version posted February 6, 2021. The copyright holder for this preprint (which was not certified by peer review) is the author/funder, who has granted medRxiv a license to display the preprint in perpetuity. It is made available under a CC-BY 4.0 International license .

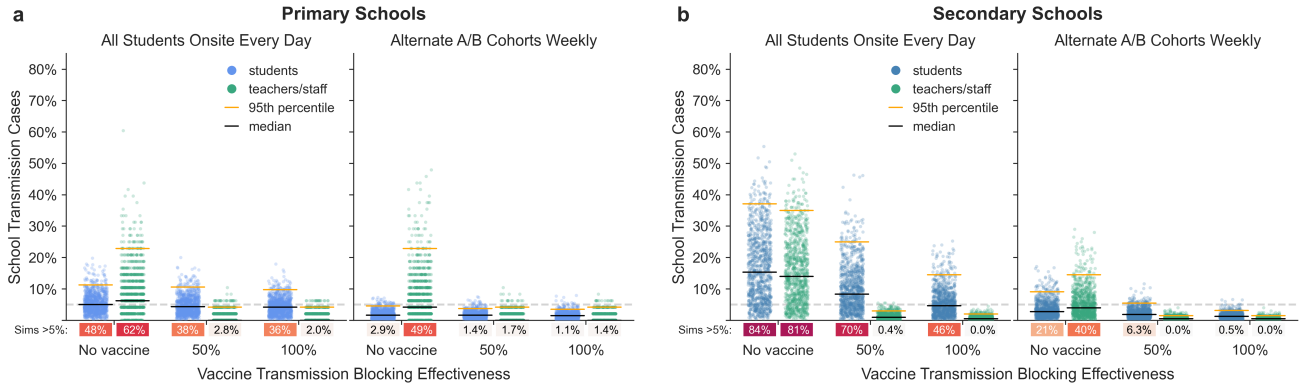

Figure 7: Effects of vaccinating teachers. The distributions of school transmission events as a percentage of school population for 1,000 simulations with vaccination of teachers and staff in (**a**) primary schools and (**b**) secondary schools. Results are shown for scenarios with R_0=1.5, approximately weekly new case introductions, and no testing. We compare vaccines that block transmission fully (100% reduction) with ones that block partially (50% reduction) and with no vaccination at all. Because vaccination is only 90% effective, some teachers and staff become infected even when all are vaccinated.

protected against infection (Figure 7). Vaccinating teachers with a transmission-blocking vaccine also reduces the risk of outbreaks among students, particularly when paired with cohorting. The combination of vaccinating teachers and cohorting students continues to substantially reduce the risk of outbreaks at higher levels of transmissibillity (Supporting Figures), which suggests this strategy may offer a proactive defense against the spread of more transmissive variants, provided that vaccines remain effective against such strains. While vaccination benefits those who have been vaccinated and facilitates reopening overall, maintaining additional interventions will be particularly important if vaccines do not fully block transmission.

Limitations

Like all epidemiological models, ours is a simplification of a complex, highly variable world. Our model is built on a series of assumptions and parameters; To the degree that these do not accurately reflect the real world, the model will be ineffective at predicting even the range of possible outcomes. We have attempted to account for uncertainty by embracing realistic heterogeneity and stochasticity in our model and by evaluating the sensitivity of outcomes across plausible ranges of values for critical parameters (see the Supporting Figures). Still, in a novel pandemic where many epidemiological parameters remain uncertain, and social and behavioral factors are fluid, some mismatch is inevitable.

The basic reproduction number (R_0)—the average number of new cases generated by an infectious individual in a fully susceptible population—is a critical driver of disease dynamics. In recent months, R_0 has ranged between 0.75–1.2 for many communities in the United States (46). This reflects an average rate of transmission integrated over many contexts and behaviors, including aggressive and widespread efforts to curtail transmission, such as social distancing, restricting large groups, and closing many schools, businesses, and other gathering places. Reopening schools would reintroduce settings where large numbers of individuals interact, and average rates of transmission could be higher in schools than in the overall community. Still, basic in-school interventions such as mask wearing, physical distancing, and behavioral changes are expected to significantly reduce R_0.

In our model, we assume that these basic interventions can reduce R_0 to 1.5, roughly half of what it would be in

medRxiv preprint doi: https://doi.org/10.1101/2021.01.22.21250282; this version posted February 6, 2021. The copyright holder for this preprint (which was not certified by peer review) is the author/funder, who has granted medRxiv a license to display the preprint in perpetuity. It is made available under a CC-BY 4.0 International license .

the absence of intervention. Previous studies suggest that transmission is relatively limited in schools (22, 37, 38, 47–49). In addition to the basic measures listed above, many of the schools described in these studies were already implementing one or more interventions along the lines of the ones we analyze here: cohorting, isolating groups, testing, contact tracing, reducing the number of people on campus, and so forth (17, 37, 49, 50). These studies largely corroborate our findings that school transmission is often kept in check when such mitigation strategies are used. Fewer studies have considered schools that are only using masks and other basic measures, but there is evidence that sizable school outbreaks can occur in these contexts (18). We find that the probability and size of outbreaks are strongly influenced by the underlying R_0, but the relative effects of mitigations are robust across a range of R_0 values (Supporting Figures).

Here we have simulated a subset of the currently practiced strategies for returning to in-person learning (51). We assume that students, teachers and school staff adhere to testing cadences, cohorting schedules, and quarantine policies in addition to basic measures. In the absence of evidence to the contrary, we assume that—holding transmissibility and susceptibility constant—all forms of close contact are equally likely to result in transmission. In practice, the nature of interpersonal relations may make transmission from student to student or from teacher to teacher more likely than transmission between these groups, and could explain why some contact-tracing studies have reported disproportionately low student-to-teacher transmission (37, 52).

We have modeled primary school children as being less susceptible to SARS-CoV-2 infection than teachers and staff. Recent evidence from seroprevalence and contact-tracing studies support this assumption (16, 20, 53–55). However, because a high percentage of children develop asymptomatic disease, COVID-19 cases among children may be more likely to go undetected. Therefore, it is possible that the apparent decreased susceptibility to SARS-CoV-2 infection among primary school-age children is an artifact of underreporting.

Over the course of the pandemic, community prevalence measurements have fluctuated substantially on a timescale of months, due to changing individual behaviors and societal interventions. Because these fluctuations have been largely unpredictable, we have elected to use a constant introduction rate throughout. In doing so we are effectively decoupling infection dynamics within the school from epidemic dynamics in the community. In our model, intervention choices that lead to a large number of school-related transmissions do not feed back on the community prevalence to influence the downstream hazard of community introduction back into the school. Similarly, in our model, mitigation choices that block school transmission do not reduce the community introduction rate. This seems reasonable when schools are not important drivers of the community prevalence of SARS-CoV-2 infection, as appears to be the case especially for K-5 schools (17, 37, 56). Where schools are important drivers of community dynamics, however, our model risks underestimating the consequences of mitigation efforts. When schools drive community prevalence, planners must also consider the cost of the additional community infections that result from reopening schools—which we have not done here.

Summary

We have presented results from a simulation model of reopening schools during the COVID-19 pandemic. The purpose of this model is to provide a scenario-simulating tool that, when used in concert along with other credible sources of information and data, can aid decisions around school reopening policies.

We attempt to make reasonable assumptions about epidemiological parameters and aspects of human behavior that drive disease transmission. Our results tend to be robust to these choices, and the qualitative findings that

medRxiv preprint doi: https://doi.org/10.1101/2021.01.22.21250282; this version posted February 6, 2021. The copyright holder for this preprint (which was not certified by peer review) is the author/funder, who has granted medRxiv a license to display the preprint in perpetuity. It is made available under a CC-BY 4.0 International license .

we report — advantages to cohorting, testing, and vaccination — are expected to hold up more broadly. In the Supporting Figures, we provide results from our model for a range of parameter combinations, including transmissibility (R_0), case introduction rates, student susceptibilities, and intervention strategies, which can be used to assist in dynamic decision-making in response to uncertain and changing local circumstances. Our online webapp (https://www.color.com/impact-of-primary-school-covid-19-testing) provides a way to explore the range of parameters interactively.

Our model suggests that dividing students into cohorts that attend school in-person on alternating schedules can be a powerful strategy for mitigating risk. Such cohorting strategies are more effective in primary schools than in secondary schools, due to classroom organization. Secondary schools could consider restructuring schedules to reduce the mixing of students between classrooms. Cohorting is effective in our model because students largely restrict in-person interactions to other individuals within their own groups, and this takes place only while at school. When students socialize across cohort boundaries outside of school—as secondary students are wont to do—the effectiveness of cohorting is reduced.

Teachers and staff are more susceptible to the virus than primary school students and at higher risk of severe disease than students of any age. Moreover, teachers serve as conduits for outbreaks to move among classrooms within the school network. Frequent, proactive testing of teachers and staff can interrupt such transmission chains and further protect them from infection.

Vaccinating teachers and staff is a powerful tool for protecting this critical workforce. If vaccines effectively block SARS-CoV-2 transmission in addition to COVID-19 symptoms, vaccinating teachers and staff can significantly dampen outbreak dynamics in both primary and secondary schools. The result would be fewer cases among adults and students alike.

The success of reopening efforts will hinge on the amount of transmission that occurs in schools. The higher the transmissibility, parameterized here as R_0, the greater the chance of substantial outbreaks in a school setting. Physical distancing, diligent use of masks, and other environmental controls offer a first-line approach to reducing transmission and will be an important component of reopening plans.

For both primary and secondary schools, the risk of an outbreak increases as cases in the surrounding community rise. One of the most effective ways to safely reopen schools is by controlling COVID-19 in the community. Surveillance should be in place to monitor levels of community transmission and schools should be prepared to respond flexibly.

Because highly transmissible variants such as B.1.1.7 pose increased risks for outbreaks, schools need to be vigilant on multiple fronts. First, where genomic surveillance is available, school districts and counties need to monitor the introduction and spread of these variants. Second, irrespective of the variants involved, it will be important to monitor epidemic dynamics within any given school and to respond quickly should uncontrolled spread take place. An additional virtue of testing is that it facilitates early detection of such events.

Our model suggests that under certain parameters, it may become difficult or impossible to keep the probability of outbreaks low across the schools of an entire district. Trip-wire strategies may be necessary, whereby school districts return to distance learning in response to worsening conditions.

While gaps remain in our understanding of transmission in school settings, both real-world experience and models — including the one presented here — suggest a path forward for schools to reopen, particularly when community transmission is low and when it is possible to deploy and consistently implement the mitigation measures we have modeled here.

medRxiv preprint doi: https://doi.org/10.1101/2021.01.22.21250282; this version posted February 6, 2021. The copyright holder for this preprint (which was not certified by peer review) is the author/funder, who has granted medRxiv a license to display the preprint in perpetuity. It is made available under a CC-BY 4.0 International license .

Acknowledgements The authors thank Martin Rosvall for help in developing the contact network structures used in the SEIRS+ model. Ted Bergstrom, Natalie Dean, Bill Hanage, Michael Lachmann, and Marc Lipsitch provided valuable feedback in developing the model and adapting it to the school scenarios considered here.

Author contributions Conceived of the model: RSM, CTB. Reviewed the literature: RSM, HEW. Parameterized the model: RSM, JRH, HEW. Implemented the model and ran the simulations: RSM, JRH. Produced the data visualizations: RSM, JRH. Analyzed the results: RSM, CTB, JRH, HEW, AYZ. Developed the interactive web app: JRH. Drafted the manuscript: CTB, RSM, HEW, JRH, AYZ.

Disclosures CTB and RSM consult for Color Health. CTB has received honoraria from Novartis. JRH, HEW and AYZ are currently employed by and have equity interest in Color Health.

References

[1] UNESCO (2020) 1.3 billion learners are still affected by school or university closures (unesco.org/news/13-billion-learners-are-still-affected-school-university-closures-educational-institutions). Accessed: 2020-11-9.

[2] Hanushek EA, Woessmann L (2020) The economic impacts of learning losses.

[3] Galloway SE (2021) Emergence of SARS-CoV-2 b.1.1.7 lineage — united states, december 29, 2020–january 12, 2021. *MMWR Morb. Mortal. Wkly. Rep.* 70.

[4] Nierenberg A, Pasick A (2020) Will any more schools reopen in 2020? *The New York Times*.

[5] Leidman E (2021) COVID-19 trends among persons aged 0–24 years — united states, march 1–december 12, 2020. *MMWR Morb. Mortal. Wkly. Rep.* 70.

[6] Giordano G, et al. (2020) Modelling the COVID-19 epidemic and implementation of population-wide interventions in italy. *Nat. Med.* 26(6):855–860.

[7] CDC (2021) COVID-19 forecasts: Deaths (https://www.cdc.gov/coronavirus/2019-ncov/covid-data/forecasting-us.html). Accessed: 2021-1-7.

[8] Ferguson NM (2020) *Report 9: Impact of Non-pharmaceutical Interventions (NPIs) to Reduce COVID19 Mortality and Healthcare Demand.* (Imperial College London).

[9] Kucharski AJ, et al. (2020) Early dynamics of transmission and control of COVID-19: a mathematical modelling study. *Lancet Infect. Dis.* 20(5):553–558.

[10] Peak CM, et al. (2020) Individual quarantine versus active monitoring of contacts for the mitigation of COVID-19: a modelling study. *Lancet Infect. Dis.* 20(9):1025–1033.

[11] Aleta A, et al. (2020) Modelling the impact of testing, contact tracing and household quarantine on second waves of COVID-19. *Nat Hum Behav* 4(9):964–971.

medRxiv preprint doi: https://doi.org/10.1101/2021.01.22.21250282; this version posted February 6, 2021. The copyright holder for this preprint (which was not certified by peer review) is the author/funder, who has granted medRxiv a license to display the preprint in perpetuity. It is made available under a CC-BY 4.0 International license .

[12] Wang X, et al. (2020) Effects of cocooning on coronavirus disease rates after relaxing social distancing. *Emerg. Infect. Dis.* 26(12):3066–3068.

[13] Bershteyn A, Kim HY, McGillen JB, Braithwaite RS (2020) Which policies most effectively reduce SARS-CoV-2 transmission in schools? *medRxiv*.

[14] Bracis C, et al. (2021) Widespread testing, case isolation and contact tracing may allow safe school reopening with continued moderate physical distancing: A modeling analysis of king county, WA data. *Infect Dis Model* 6:24–35.

[15] Bilinski AM, Salomon JA, Giardina J, Ciaranello A, Fitzpatrick M (2021) Passing the test: A model-based analysis of safe school-reopening strategies. *medRxiv*.

[16] Goldstein E, Lipsitch M, Cevik M (2020) On the effect of age on the transmission of SARS-CoV-2 in households, schools and the community. *J. Infect. Dis.*

[17] Ismail SA, Saliba V, Bernal JL, Ramsay ME, Ladhani SN (2020) SARS-CoV-2 infection and transmission in educational settings: a prospective, cross-sectional analysis of infection clusters and outbreaks in england.

[18] Stein-Zamir C, et al. (2020) A large COVID-19 outbreak in a high school 10 days after schools' reopening, israel, may 2020. *Eurosurveillance* 25(29):2001352.

[19] (2020) Covid-19 school response dashboard. Accessed: 2020-12-11.

[20] Viner RM, et al. (2020) Susceptibility to SARS-CoV-2 infection among children and adolescents compared with adults: A systematic review and meta-analysis. *JAMA Pediatr.*

[21] Assaker R, et al. (2020) Presenting symptoms of COVID-19 in children: a meta-analysis of published studies. *Br. J. Anaesth.* 125(3):e330–e332.

[22] Rajmil L (2020) Role of children in the transmission of the COVID-19 pandemic: a rapid scoping review. *BMJ Paediatr Open* 4(1):e000722.

[23] Keeling MJ, Rohani P (2011) *Modeling Infectious Diseases in Humans and Animals*. (Princeton University Press).

[24] Danon L, House TA, Read JM, Keeling MJ (2012) Social encounter networks: collective properties and disease transmission. *Journal of The Royal Society Interface* 9(76):2826–2833. Publisher: Royal Society.

[25] Badham J, Stocker R (2010) The impact of network clustering and assortativity on epidemic behaviour. *Theoretical Population Biology* 77(1):71–75.

[26] Endo A, Abbott S, Kucharski A, Funk S (2020) Estimating the overdispersion in COVID-19 transmission using outbreak sizes outside china. wellcome open research, 5 (67).

[27] Adam D, et al. (2020) Clustering and superspreading potential of severe acute respiratory syndrome coronavirus 2 (SARS-CoV-2) infections in hong kong.

medRxiv preprint doi: https://doi.org/10.1101/2021.01.22.21250282; this version posted February 6, 2021. The copyright holder for this preprint (which was not certified by peer review) is the author/funder, who has granted medRxiv a license to display the preprint in perpetuity. It is made available under a CC-BY 4.0 International license .

[28] Li Q, et al. (2020) Early transmission dynamics in wuhan, china, of novel Coronavirus-Infected pneumonia. *N. Engl. J. Med.* 382(13):1199–1207.

[29] (2020) Royal society publishes rapid review of the science of the reproduction number and growth rate of COVID-19 (https://royalsociety.org/news/2020/09/set-c-covid-r-rate/). Accessed: 2021-1-17.

[30] Read JM, Bridgen JRE, Cummings DAT, Ho A, Jewell CP (2020) Novel coronavirus 2019-nCoV: early estimation of epidemiological parameters and epidemic predictions.

[31] CDC (2020) Healthcare workers (https://www.cdc.gov/coronavirus/2019-ncov/hcp/planning-scenarios.html). Accessed: 2021-1-17.

[32] Liu Y, Gayle AA, Wilder-Smith A, Rocklöv J (2020) The reproductive number of COVID-19 is higher compared to SARS coronavirus. *J. Travel Med.* 27(2).

[33] CDC (2020) Options to reduce quarantine for contacts of persons with SARS-CoV-2 infection using symptom monitoring and diagnostic testing (https://www.cdc.gov/coronavirus/2019-ncov/more/scientific-brief-options-to-reduce-quarantine.html). Accessed: 2020-12-16.

[34] Korber B, et al. (2020) Tracking changes in SARS-CoV-2 spike: Evidence that D614G increases infectivity of the COVID-19 virus. *Cell* 182(4):812–827.e19.

[35] Leung K, Shum MH, Leung GM, Lam TT, Wu JT (2021) Early transmissibility assessment of the N501Y mutant strains of SARS-CoV-2 in the united kingdom, october to november 2020. *Euro Surveill.* 26(1).

[36] Karin O, et al. (2020) Cyclic exit strategies to suppress COVID-19 and allow economic activity.

[37] Zimmerman KO, et al. (2021) Incidence and secondary transmission of SARS-CoV-2 infections in schools. *Pediatrics*.

[38] Kampe EOi, Lehfeld AS, Buda S, Buchholz U, Haas W (2020) Surveillance of COVID-19 school outbreaks, germany, march to august 2020. *Eurosurveillance* 25(38):2001645.

[39] Larremore DB, et al. (2020) Test sensitivity is secondary to frequency and turnaround time for COVID-19 screening. *Sci Adv*.

[40] Denny TN, et al. (2020) Implementation of a pooled surveillance testing program for asymptomatic SARS-CoV-2 infections on a college campus - duke university, durham, north carolina, august 2-october 11, 2020. *MMWR Morb. Mortal. Wkly. Rep.* 69(46):1743–1747.

[41] Bergstrom T, Bergstrom CT, Li H (2020) Frequency and accuracy of proactive testing for COVID-19.

[42] (2020) Return to on-site sars-cov-2 testing protocols.

[43] Polack FP, et al. (2020) Safety and efficacy of the BNT162b2 mRNA covid-19 vaccine. *N. Engl. J. Med.* 383(27):2603–2615.

[44] Baden LR, et al. (2020) Efficacy and safety of the mRNA-1273 SARS-CoV-2 vaccine. *N. Engl. J. Med.*

medRxiv preprint doi: https://doi.org/10.1101/2021.01.22.21250282; this version posted February 6, 2021. The copyright holder for this preprint (which was not certified by peer review) is the author/funder, who has granted medRxiv a license to display the preprint in perpetuity. It is made available under a CC-BY 4.0 International license .

[45] (2020) Teachers should be prioritized for vaccination against COVID-19 (https://www.unicef.org/press-releases/teachers-should-be-prioritized-vaccination-against-covid-19). Accessed: 2021-1-18.

[46] Abbott S, et al. (2020–2021) Temporal variation in transmission during the covid-19 outbreak. *CMMID Repository*.

[47] Ismail SA, Saliba V, Bernal JL, Ramsay ME, Ladhani S (2020) SARS-CoV-2 infection and transmission in educational settings: Cross-Sectional analysis of clusters and outbreaks in england.

[48] Heavey L, Casey G, Kelly C, Kelly D, McDarby G (2020) No evidence of secondary transmission of COVID-19 from children attending school in ireland, 2020. *Euro Surveill.* 25(21).

[49] Macartney K, et al. (2020) Transmission of SARS-CoV-2 in australian educational settings: a prospective cohort study. *Lancet Child Adolesc Health* 4(11):807–816.

[50] Panovska-Griffiths J, et al. (2020) Determining the optimal strategy for reopening schools, the impact of test and trace interventions, and the risk of occurrence of a second COVID-19 epidemic wave in the UK: a modelling study. *Lancet Child Adolesc Health* 4(11):817–827.

[51] CDC (2020) Operating schools during COVID-19 (https://www.cdc.gov/coronavirus/2019-ncov/community/schools-childcare/schools.html). Accessed: 2021-1-7.

[52] Gillespie DL ea (2021) The experience of two independent schools with in-person learning during the covid-19 pandemic. *In press, Journal of School Health*.

[53] Carsetti R, et al. (2020) The immune system of children: the key to understanding SARS-CoV-2 susceptibility? *Lancet Child Adolesc Health* 4(6):414–416.

[54] Bunyavanich S, Do A, Vicencio A (2020) Nasal gene expression of Angiotensin-Converting enzyme 2 in children and adults. *JAMA* 323(23):2427–2429.

[55] Leeb RT, et al. (2020) COVID-19 trends among School-Aged children - united states, march 1-september 19, 2020. *MMWR Morb. Mortal. Wkly. Rep.* 69(39):1410–1415.

[56] Brandal LT, et al. (2021) Minimal transmission of SARS-CoV-2 from paediatric COVID-19 cases in primary schools, norway, august to november 2020. *Euro Surveill.* 26(1).

[57] Krylova O, Earn DJD (2013) Effects of the infectious period distribution on predicted transitions in childhood disease dynamics.

[58] Feng Z, Xu D, Zhao H (2007) Epidemiological models with non-exponentially distributed disease stages and applications to disease control. *Bull. Math. Biol.* 69(5):1511–1536.

[59] Fagnan J, Abnar A, Rabbany R, Zaiane OR (2018) Modular Networks for Validating Community Detection Algorithms. *arXiv:1801.01229 [physics]*. arXiv: 1801.01229.

[60] Newman MEJ, Park J (2003) Why social networks are different from other types of networks. *Physical Review E* 68(3).

medRxiv preprint doi: https://doi.org/10.1101/2021.01.22.21250282; this version posted February 6, 2021. The copyright holder for this preprint (which was not certified by peer review) is the author/funder, who has granted medRxiv a license to display the preprint in perpetuity. It is made available under a CC-BY 4.0 International license .

[61] Read JM, Eames KT, Edmunds WJ (2008) Dynamic social networks and the implications for the spread of infectious disease. *Journal of The Royal Society Interface* 5(26):1001–1007.

[62] Salathe M, et al. (2010) A high-resolution human contact network for infectious disease transmission. *Proceedings of the National Academy of Sciences* 107(51):22020–22025.

[63] Barclay VC, et al. (2014) Positive Network Assortativity of Influenza Vaccination at a High School: Implications for Outbreak Risk and Herd Immunity. *PLoS One* 9(2).

[64] Levine-Tiefenbrun M, et al. (2020) Association of covid-19 rt-qpcr test false-negative rate with patient age, sex and time since diagnosis. *medRxiv*.

[65] CDC (2020) Duration of isolation and precautions for adults with COVID-19 (https://www.cdc.gov/coronavirus/2019-ncov/hcp/duration-isolation.html). Accessed: 2020-12-16.

medRxiv preprint doi: https://doi.org/10.1101/2021.01.22.21250282; this version posted February 6, 2021. The copyright holder for this preprint (which was not certified by peer review) is the author/funder, who has granted medRxiv a license to display the preprint in perpetuity. It is made available under a CC-BY 4.0 International license .

Appendix A Model Description

Contents

A.1 SEIRS+ Extended SEIR Network Model . . . 18
A.1.1 Heterogeneity . . . 18
A.1.2 Compartments . . . 19
A.1.3 Dynamics . . . 20
A.1.4 Transmission . . . 20
A.1.4.1 Global transmission . . . 21
A.1.4.2 Local transmission . . . 21
A.2 School Models . . . 22
A.2.1 Disease progression parameters . . . 22
A.2.2 Transmission parameters . . . 23
A.2.3 Contact Networks . . . 26
A.2.3.1 Primary school contact networks . . . 26
A.2.3.2 Secondary school contact networks . . . 26
A.2.3.3 Quarantine contact networks . . . 26
A.2.3.4 Weekend contact networks . . . 27
A.2.3.5 Cohort contact networks . . . 27
A.2.4 Case Introductions . . . 32
A.2.5 Interventions . . . 33
A.2.5.1 Simulation loop . . . 33
A.2.5.2 Testing . . . 34
A.2.5.3 Cohorting . . . 35
A.2.5.4 Isolation . . . 36
A.2.5.5 Vaccination . . . 37

A.1 SEIRS+ Extended SEIR Network Model

SEIRS+ is an open source Python framework developed by McGee et al. that supports flexible parameterization and implementation of sophisticated epidemiological models (https://github.com/ryansmcgee/seirsplus). The models studied in this work are parameterizations of the stochastic Extended SEIR Network Model provided in the SEIRS+ framework. We simulate our models using the Interventions Simulation Loop provided in SEIRS+ with minor modifications for our particular school context. Extensive documentation for the models, simulation loops, and other features of SEIRS+ can be found on the SEIRS+ github wiki (https://github.com/ryansmcgee/seirsplus/wiki).

A.1.1 Heterogeneity

In the SEIRS+ Extended SEIR Network Model, individuals are represented as nodes in a contact network, and all parameters, interactions, and interventions can be specified on a node-by-node basis. Therefore, this model enables explicit representation of heterogeneity in disease characteristics, contact patterns, and behaviors, which

medRxiv preprint doi: https://doi.org/10.1101/2021.01.22.21250282; this version posted February 6, 2021. The copyright holder for this preprint (which was not certified by peer review) is the author/funder, who has granted medRxiv a license to display the preprint in perpetuity. It is made available under a CC-BY 4.0 International license .

are important for modeling small, age-stratified populations such as schools. Parameter choices and distributions for our school models are described in the School Models appendix section.

A.1.2 Compartments

The Extended SEIR Network Model extends the classic SEIR model of infectious disease to represent pre-symptomatic, asymptomatic, and symptomatic disease states, which are of particular relevance to the SARS-CoV-2 pandemic. The classic SEIR model divides the population into susceptible (S), exposed (E), infectious (I), and recovered (R) individuals. In this extended model, the infectious subpopulation is further subdivided into pre-symptomatic (I_{pre}), asymptomatic (I_{asym}), and symptomatic (I_{sym}) compartments, all of which represent contagious individuals (the full Extended SEIR Network Model includes a hospitalized infectious state, but we assume no hospitalization in this report and effectively ignore this compartment). Individuals transition from one compartment to the next at times determined by the disease characteristics (see Appendix A.2.1 Disease progression parameters). A parameterizable fraction of the population are deemed asymptomatic and will progress to the asymptomatic compartment when exiting the presymptomatic compartment, while the remainder of the population will progress to the symptomatic compartment. The dynamics of compartment transitions are described further in the Dynamics appendix section.

The effect of isolating individuals in response to symptoms or testing is modeled by introducing compartments that represent quarantined individuals (Figure Figure A1). An individual may be quarantined in any disease state, and every disease state has a corresponding quarantine compartment. Quarantined individuals follow the same progression through the disease states, but their set of close contacts are defined by a distinct quarantine contact network (Appendix A.2.3 Contact Networks). In this work, individuals are moved into quarantine states by the Intervention Simulation Loop (Appendix A.2.5.1), such as when a positive test result is returned, as opposed to according to a transition rate. Individuals remain in the quarantine compartment flow until the designated isolation period has been reached (10 days in this work), at which time they are moved into the non-quarantine compartment

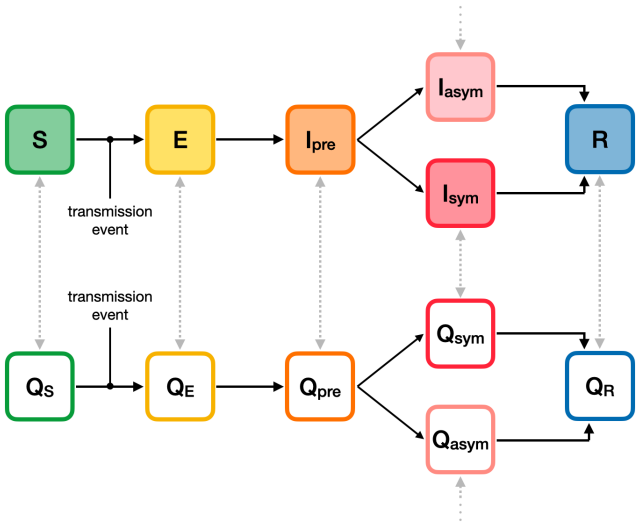

Figure A1: Compartment model. The compartment model that defines the progression of disease states in the Extended SEIR Network Model.

medRxiv preprint doi: https://doi.org/10.1101/2021.01.22.21250282; this version posted February 6, 2021. The copyright holder for this preprint (which was not certified by peer review) is the author/funder, who has granted medRxiv a license to display the preprint in perpetuity. It is made available under a CC-BY 4.0 International license .

corresponding to their current disease state.

A.1.3 Dynamics

Transmission dynamics are simulated using the Gillespie algorithm, a common and rigorous method for simulating stochastic interaction dynamics. Briefly, the system's differential equations are adapted to compute the 'propensity' of the possible events (i.e., the expected amount of time until a given event will take place) for all nodes at each time step. These propensities are then used to compute the probabilities of all possible state events normalized across the entire population. A random node and corresponding transition are selected to execute according to these probabilities in each time step. The propensities of transmission events (S to E transitions) are proportional to the product of the prevalence of infectious individuals among each node's contacts and the transmissibilities and susceptibilities of the interacting individuals (see Appendix A.1.4 Transmission).

SEIRS+ supports calculating the propensities of disease progression transitions (e.g., E to I_{pre}, Q_{pre} to Q_{sym}) in two different ways: 1) using transition rates (standard Gillespie implementation), or 2) using compartment residence times. Running the model in the first mode results in exponentially distributed residence times in each compartment, as in classic mass action SEIR-like models. In the latter mode, each individual is assigned a residence time for each compartment, and the propensity for a given individual to transition out of the current state is 0 until this residence period has elapsed, at which time this propensity becomes large such that the next event will be this given individual transitioning to the next compartment with probability approaching 1. This results in a hybrid model where transmission events occur stochastically according to the Gillespie algorithm while other disease progression transitions occur in a clock-like manner in parallel. In reality, residence times in each disease state are not exponentially distributed, and the discrepancies can be particularly important when looking at early stages of an outbreak and when considering control strategies such as proactive testing (57, 58). As such, we use the residence time propensity calculation mode in this work and assign heterogeneous residence times to individuals drawn from gamma distributions that better match empirical descriptions of the disease dynamics for COVID-19 (Appendix A.2.1).

For more information about the propensity equations, refer to https://github.com/ryansmcgee/seirsplus/wiki.

A.1.4 Transmission

The dynamics governing transmission events that cause susceptible individuals to become exposed are arguably the most important to understand in any epidemiological model, so we break down the transmission dynamics of the Extended SEIR Network Model in detail here.

In general, the propensity $P^{(i)}(S \rightarrow E)$ of a given susceptible individual i becoming infected is proportional to the product of the prevalence of infectious individuals among their contacts, the average transmissibility of their infectious contacts $\overline{\beta}^{(\text{contacts})}$, and their own susceptibility to infection $\alpha^{(i)}$.

$$P^{(i)}(S \rightarrow E) \propto \alpha^{(i)} \times \overline{\beta}^{(\text{contacts})} \times (\text{prevalence among contacts})$$

An individual's transmissibility $\beta^{(i)}$ (i.e., transmission rate) is equal to the expected number of cases that this individual would generate in a fully-susceptible population (i.e., the reproduction number for the individual, $R_0^{(i)}$ divided by the length of their infectious period $\gamma^{(i)}$.

$$\beta^{(i)} = \frac{R_0^{(i)}}{\gamma^{(i)}}$$

medRxiv preprint doi: https://doi.org/10.1101/2021.01.22.21250282; this version posted February 6, 2021. The copyright holder for this preprint (which was not certified by peer review) is the author/funder, who has granted medRxiv a license to display the preprint in perpetuity. It is made available under a CC-BY 4.0 International license .

For the purposes of the models considered in this work, the propensity of a given individual i becoming infected is calculated using the following equation[1], which we will break down in the rest of this section

$$P^{(i)}(S \to E) = \alpha^{(i)} \left[p \underbrace{\left(\frac{\bar{\beta}\left(I_{\text{pre}} + I_{\text{sym}} + I_{\text{asym}}\right)}{N} \right)}_{\text{global transmission}} + (1-p) \underbrace{\left(\frac{\sum_{j \in C_G^{(i)}} \delta^{(ji)} \left(\beta^{(ji)} \mathbf{1}_{X^{(j)} \in \{I_{\text{pre}}, I_{\text{sym}}, I_{\text{asym}}\}} \right)}{|C_G^{(i)}|} \right)}_{\text{local transmission}} \right]$$

In this model, disease transmission may occur either from close contacts defined by the contact network structure or from casual contacts. Close contacts are individuals with whom one has repeated, sustained, or close proximity interactions on a regular basis: classmates, friends, housemates, or other close relationships. In contrast, casual contacts are individuals with whom one has incidental, brief, or superficial contact on an infrequent basis and to whom one is not connected directly on the network. A network locality parameter p sets the relative frequency and weight of transmission among close (local network) and casual (global) contacts in the model population.

A.1.4.1 Global transmission A fraction p of a given individual's interactions are with casual contacts, which are assumed to be individuals randomly sampled from the population at large, irrespective of the contact network. With respect to these global interactions, every node in the population is equally likely to come into contact with every other node, and the population can be considered well-mixed. Thus the propensity of global transmission is calculated in the same way as mass action compartment models that assume a well-mixed population. The propensity for a given susceptible individual to become exposed due to global transmission is proportional to the product of that individual's susceptibility $\alpha^{(i)}$, the population mean transmissibility of infectious individuals $\overline{\beta}$, and the prevalence of infectious individuals in the overall population $(I_{\text{pre}} + I_{\text{sym}} + I_{\text{asym}})/N$.

A.1.4.2 Local transmission A fraction $1-p$ of a given individual's interactions are with individuals from their set of "close contacts." An individual's close contacts are defined as the nodes adjacent to the given node in the contact network ($C_G^{(i)}$ denotes the set of close contacts for individual i: the nodes adjacent to node i in the contact network graph G). With respect to local transmission, transmissibility is considered on a pairwise basis. That is, every directed edge of the contact network representing transmission from infected node j to susceptible node i is assigned a transmissibility weight $\beta^{(ji)}$. The transmissibility of such an interaction is assumed to be equal to the transmissibility of the infected individual (i.e., $\beta^{(ji)} = \beta^{(j)}$). The propensity for a given susceptible individual to become exposed due to local transmission is calculated as the product of that individual's susceptibility and the sum transmissibility of their infectious close contacts ($\mathbf{1}_{X^{(j)} \in \{I_{\text{pre}}, I_{\text{sym}}, I_{\text{asym}}\}}$ is an indicator function that takes the value 1 when the state $X^{(j)}$ of the contact node j is one of the infectious states and 0 otherwise), divided by the size of their local network ($|C_G^{(i)}|$ denotes the size of the set of close contacts for individual i).

This amounts to the propensity of exposure for node i being proportional to the product of their susceptibility and the transmissibility-weighted prevalence of infectious individuals in their local network. Thus, propensity for exposure due to local transmission is frequency dependent and analogous to the propensity contribution from

[1] This equation is simplified from the general equation implemented in the Extended SEIR Network Model, which includes parameters and terms that are not used here and are thus zeroed out.

medRxiv preprint doi: https://doi.org/10.1101/2021.01.22.21250282; this version posted February 6, 2021. The copyright holder for this preprint (which was not certified by peer review) is the author/funder, who has granted medRxiv a license to display the preprint in perpetuity. It is made available under a CC-BY 4.0 International license .

global transmission. Implicit in this formulation is an assumption that all individuals have an equal interaction budget (e.g., equal amount of time or intensity interacting with others), and individuals with more close contacts (i.e., higher degree) interact less with each contact and are therefore less likely to become exposed by any single individual. An additional factor $\delta^{(ji)}$ appears in the calculation of propensity for exposure due to local transmission. This pairwise factor is used to re-weight the transmissibility of interactions according to the connectivity of the interacting individuals. Here we are interested in re-weighting in order to counteract, in part, the aforementioned implicit assumption that all individuals have an equal interaction budget. While it is reasonable to think that individuals (e.g., secondary school teachers) who have many contacts (e.g., students) do not interact as closely with each of their contacts as another individual who only has a handful of contacts, we do not assume that the propensity of infection decreases linearly with degree for SARS-CoV-2 transmission. We define the degree scaling factor $\delta^{(ji)}$ as

$$\delta^{(ji)} = \frac{\log(D^{(i)}) + \log(D^{(j)})}{2\log(\overline{D})}$$

where $D^{(j)}$ and $D^{(i)}$ are the degrees of nodes j and i, respectively, and $\overline{D}$ is the mean degree of the network. Using this definition of $\delta^{(ji)}$, when two individuals whose average degree is an order of magnitude greater than the average degree of the population overall, then the propensity of exposure in their interaction is twice that of two averagely-connected individuals. Thus, the propensity for infection by a single infectious contact is lower for highly-connected individuals compared to low connectivity individuals, but not proportionally so.

A.2 School Models

The following sections describe the specific assumptions and parameter values used to define the primary and secondary school models studied in this work. These models were implemented using the SEIRS+ framework's Extended SEIR Network Model (see Appendix A.1 SEIRS+ Extended SEIR Network Model).

A.2.1 Disease progression parameters

As described in Appendix A.1.3 Dynamics, individuals remain in each compartment (excluding Susceptible) for a designated period of time before progressing to the next disease state. The population is heterogeneous for each disease state period, with each individual being assigned disease state periods drawn from gamma distributions that are informed by empirical studies of COVID-19 progression. Refer to Table A.2.1 for more information about each distribution. We assume that the distributions of disease state periods are the same for all age groups and for both quarantined and non-quarantined individuals. The same gamma distribution parameters are used to define the period probability distributions in every simulation, but the period values are randomly drawn and assigned in each replicate.

Additionally, we assume that 30% of adults and secondary school students are asymptomatic, and that 40% of primary school students (young children) are asymptomatic. In the initialization of each simulation, each individual in the population is randomly assigned a symptomatic or asymptomatic status according to these probabilities. If an individual becomes infected, they will progress to the symptomatic (I_{sym}) or asymptomatic (I_{asym}) state when exiting the pre-symptomatic (I_{pre}) state according to this assigned status. 20% of symptomatic individuals self-isolate upon entering the symptomatic state, but there are no other parameter differences between symptomatic and asymptomatic individuals in our model.

medRxiv preprint doi: https://doi.org/10.1101/2021.01.22.21250282; this version posted February 6, 2021. The copyright holder for this preprint (which was not certified by peer review) is the author/funder, who has granted medRxiv a license to display the preprint in perpetuity. It is made available under a CC-BY 4.0 International license .

A.2.2 Transmission parameters

As described in Appendix A.1.4 Transmission, the propensity of transmission events depend on the transmissibility and susceptibility parameters of interacting individuals. Each individual is assigned an individual reproduction number $R_0^{(i)}$, which is the expected number of secondary cases that the individual generates when infectious in a fully susceptible pouplation. Each individual reproduction number is converted to an individual transmissibility (i.e., transmission rate) parameter using the following standard formula

$$\beta^{(i)} = \frac{R_0^{(i)}}{\gamma^{(i)}},$$

where $\gamma^{(i)}$ is the total infectious period for individual i. We assume that individual transmissibility is heterogeneous and follows an overdispersed (long-tailed) distribution that corresponds approximately to 20% of individuals contributing 80% of the total expected number of secondary cases (the 80/20 rule). We calibrate the individual reproduction number distribution such that its mean corresponds to a chosen average basic reproduction number R_0 for the population (R_0=1.5 and R_0=2.25 are considered in the main text) and so that 80% of the weight falls in the upper 20th percentile of individuals in the tail of the distribution. Therefore, for any R_0 considered in this paper, many individuals are expected to generate fewer than 1 secondary case while a minority of individuals are expected to contribute a large number. Refer to Table A.2.2 for more information about these distributions. We assume that all age groups have transmissibilities drawn from the same distribution. In addition, we assume there is no difference in transmissibility between the pre-symptomatic, symptomatic, and asymptomatic states (i.e., the same individual transmissibility is used while an individual is in any one of these states).

Additionally, individuals are assigned a susceptibility parameter value, which weights the propensity that they become infected by any infectious contacts they may have (see Appendix A.1.4 Transmission). Adults and secondary students are assigned the baseline susceptibility value of 1.0, and thus their propensity of infection is based on the unweighted transmissibilities of their contacts. In the main text, primary school students (young children) are assumed to be 60% as susceptible as adults. Therefore, primary school students are assigned a susceptibility value of 0.6, and their propensity of infection is only 60% of that of an adult in the same infectious contact context.

We assume that 80% of transmission is attributable to close contacts (local transmission on the contact network) and 20% is attributable to casual contacts (i.e., global transmission among the overall population)(see Appendix A.1.4 Transmission). Global transmission can be thought to represent both casual interactions among members of the school population while on campus as well as relatively infrequent interactions among members of the school population while off campus (e.g., on weekends and off-cohort days).

medRxiv preprint doi: https://doi.org/10.1101/2021.01.22.21250282; this version posted February 6, 2021. The copyright holder for this preprint (which was not certified by peer review) is the author/funder, who has granted medRxiv a license to display the preprint in perpetuity. It is made available under a CC-BY 4.0 International license .

Table A.2.1 A representative distribution of period values drawn for a secondary school with 1,000 individuals is shown for each parameter in the center column below. Statistics across all replicate distributions in our analysis are shown in the rightmost column.

Disease state period	Distribution	Statistics
Latent period (time in E state)	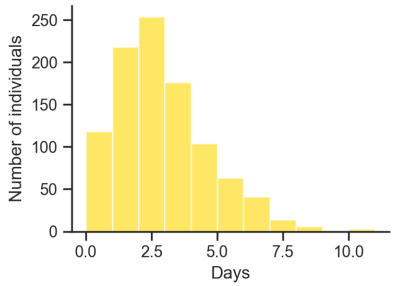 `gamma(mean=3.0, CV=0.6)`	mean 3.0 days std 1.8 days 95% CI (0.6, 7.4)
Pre-symptomatic period (time in I_{pre} state)	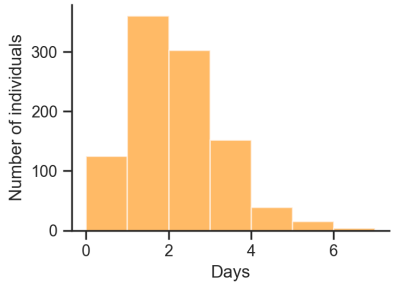 `gamma(mean=2.2, CV=0.5)`	mean 2.2 days std 1.1 days 95% CI (0.6, 4.8)
Symptomatic period (time in I_{sym} or I_{asym} state)	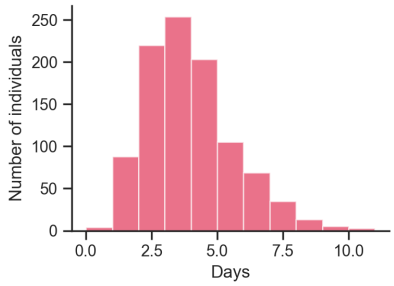 `gamma(mean=4.0, CV=0.4)`	mean 4.0 days std 1.6 days 95% CI (1.5, 7.6)
Total infectious period (total time in I_{pre}, I_{sym}, and I_{asym} states)	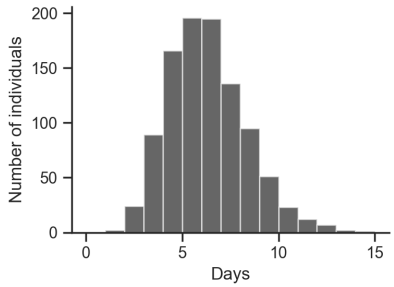 `gamma(mean=2.2, CV=0.5)`	mean 6.2 days std 1.9 days 95% CI (3.0, 10.5)

medRxiv preprint doi: https://doi.org/10.1101/2021.01.22.21250282; this version posted February 6, 2021. The copyright holder for this preprint (which was not certified by peer review) is the author/funder, who has granted medRxiv a license to display the preprint in perpetuity. It is made available under a CC-BY 4.0 International license .

Table A.2.2 A representative distribution of drawn individual reproduction number values for a secondary school with 1,000 individuals is shown for the basic reproduction numbers considered in the main text below. Statistics across all replicate distributions in our analysis are shown in the rightmost column.

Population R_0	**Distribution of individual reproduction numbers** $R_0^{(i)}$	**Statistics**
R_0 = 1.5	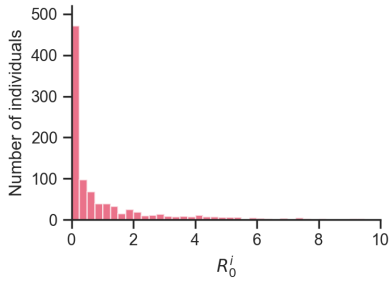 `gamma(mean=1.5, CV=2.0)`	mean 1.5 std 3.0 median 0.26 95% CI (0, 10.2) 80th percentile: 2.2 31% of values > 1.0
R_0 = 2.25	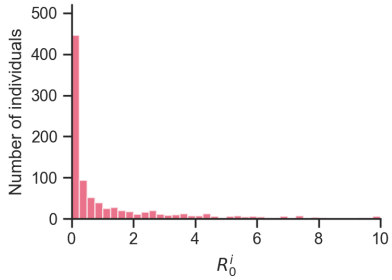 `gamma(mean=2.25, CV=2.0)`	mean 2.25 std 4.5 median 0.39 95% CI (0, 15.45) 80th percentile: 3.3 38% of values > 1.0

medRxiv preprint doi: https://doi.org/10.1101/2021.01.22.21250282; this version posted February 6, 2021. The copyright holder for this preprint (which was not certified by peer review) is the author/funder, who has granted medRxiv a license to display the preprint in perpetuity. It is made available under a CC-BY 4.0 International license .

A.2.3 Contact Networks

The SEIRS+ Extended SEIR Network Model allows arbitrary graphs to be used to specify the contact network that defines close contacts for local transmission (see Appendix A.1.4 Transmission). Here we define distinct networks representing the contact structure of a primary school and a secondary school.

A.2.3.1 Primary school contact networks For our primary school model, we simulate a medium-sized school of 480 students with 24 teachers and 24 additional staff. Each class comprises one teacher and 20 students in mutual contact. That is, the students and teacher for each classroom are strongly connected. Additionally, each teacher interacts with a handful of other teachers and staff, and students that share the same household are connected (the percentage of primary school aged children that share a household with another primary school aged child is calibrated by US census data). Most of the contacts that an individual makes in the school population are with the students and teacher in their own class, and disease transmission within a class is more likely than between classes. The FARZ algorithm, which generates random networks with built-in community structure and broad, heavy-tailed degree distributions that are realistic for human contact networks (24, 25, 59–61). Refer to Table A.2.3a for more information about the parameterization of these networks, and see Table A.2.3b for more information about the their degree and other network properties.

A.2.3.2 Secondary school contact networks For our secondary school model, we consider a medium-sized school with 800 students (200 per graduating class), 125 teachers, and 75 staff. We generate network layers for students and teachers and staff using the FARZ network generation algorithm, which allows us to calibrate epidemiologically-important network properties (e.g., cluster structure, assortativity, and clustering coefficient) to values consistent with studies of secondary school contact networks (62, 63). A FARZ network layer is generated for each grade, with students belonging to one or more social groups (i.e., network clusters) of about 10 individuals each. 80% of each student's contacts are with students in the same grade, and 80% of those within-grade contacts are with students in their own social groups. Students that share a household are connected as well (the percentage of secondary school aged children that share a household with another secondary school aged child is calibrated by US census data). Interactions between teachers and staff are represented by another FARZ network layer. Finally, students are connected with six random teachers with whom they have classes. Each teacher is associated with a grade level, and students take classes with teachers in their own grade level 75% of the time, which leads to students in the same grade being more likely to share teachers. A unique random network is generated as described for each simulation replicate. Refer to Table A.2.3c for more information about the parameterization of these networks, and see Table A.2.3d for more information about the their degree and other network properties.

A.2.3.3 Quarantine contact networks When individuals are in quarantine, a separate quarantine contact network is referenced when calculating propensities of transmission involving that individual. Here we define the contact network as the school contact network minus all edges except for connections between housemates. That is, a quarantined individual makes contact with their housemates (e.g., siblings) but no one else from the school population. Global transmission is set to 0 for individuals in quarantine as well.

medRxiv preprint doi: https://doi.org/10.1101/2021.01.22.21250282; this version posted February 6, 2021. The copyright holder for this preprint (which was not certified by peer review) is the author/funder, who has granted medRxiv a license to display the preprint in perpetuity. It is made available under a CC-BY 4.0 International license .

A.2.3.4 Weekend contact networks The contact network that is in effect on weekends is the same as the quarantine network. That is, individuals only have direct contacts with housemates on weekends. However, global transmission is left at 20% for non-quarantined individuals on weekends to represent general mixing among the school population when out of school.

A.2.3.5 Cohort contact networks One of the mitigations we consider is student cohorting, in which students are divided into two groups, only one of which attends school on any given day (see Appendix A.2.5.3 Cohorting). In our model, cohorting is implemented by alternating between two modified school contact networks (**??**). Students are divided into two cohorts, A and B. Primary students are divided such that exactly half of each classroom is in each cohort. Secondary school students are arbitrarily divided (even and odd node indexes). A modified contact network is then generated to represent when cohort A is onsite, and one is generated to represent when cohort B is onsite. Each cohort network removes all edges from offsite students, except for their household connections, while maintaining the edges of onsite students. These networks are alternated according to the given cohorting schedule, when applicable.

The degree-based pairwise transmissibility factors $\delta^{(ji)}$ (See Appendix A.1.4.2 Local transmission for details) are calculated according the the connectivities of individuals in the baseline, "everyone onsite" network. The same set of factors derived from this baseline are used to calculate the propensities of local transmission at all times (i.e., for all school days, weekend days, and cohorting days), regardless of which cohort or weekend network is being used to define the structure of close contacts. This reflects an assumption that, for example, the interactions between individuals who are on campus don't become more intense under cohorting just because fewer students are on campus.

medRxiv preprint doi: https://doi.org/10.1101/2021.01.22.21250282; this version posted February 6, 2021. The copyright holder for this preprint (which was not certified by peer review) is the author/funder, who has granted medRxiv a license to display the preprint in perpetuity. It is made available under a CC-BY 4.0 International license .

Table A.2.3a Parameters for the generation of primary school contact networks.

Parameter	**Value**	**Additional description**
Number of grades	6 (K-5)	
Number of classes per grade	4	
Number of students per class	20	
Number of teachergroups	1	FARZ parameter for teacher/staff layers: Number of network clusters in teacher/staff layer
Teacher/staff mean degree	5	Average number of connections each teacher/staff makes with other teachers/staff
`alpha`	5	FARZ parameter for teacher/staff layers: Strength of common neighbor's effect on edge formation (tunes transitivity, clustering)
`gamma`	5	FARZ parameter for teacher/staff layers: Strength of degree similarity effect on edge formation (tunes assortativity)

medRxiv preprint doi: https://doi.org/10.1101/2021.01.22.21250282; this version posted February 6, 2021. The copyright holder for this preprint (which was not certified by peer review) is the author/funder, who has granted medRxiv a license to display the preprint in perpetuity. It is made available under a CC-BY 4.0 International license .

Table A.2.3b Degree distribution plots for a representative primary school network and network property statistics averaged across all primary school contact networks used in our analysis.

Network	Degree distribution	Network properties
Overall network	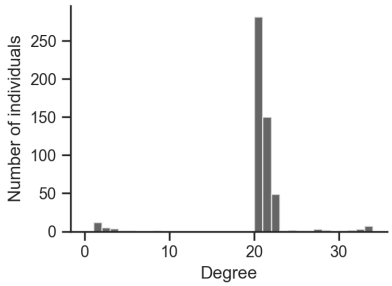	Degree mean: 20.1 Degree std: 4.5 Degree CV^2: = 0.5 Degree assortativity: 0.20 Clustering coeff.: 0.91 Average path length: 3.6
Student-Student layer	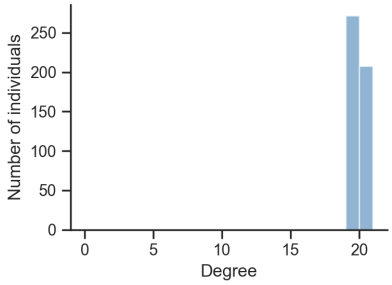	Degree mean: 19.5 Degree std 0.6 Degree CV^2 = 0.0 Degree assortativity: 0.05 Clustering coeff.: 0.95 Average path length: 3.9
Teacher-Staff layer	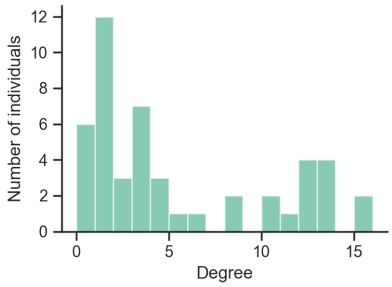	Degree mean 5.0 Degree std 4.8 Degree CV^2 = 0.8 Degree assortativity: 0.46 Clustering coeff.: 0.49 Average path length: 3.6

medRxiv preprint doi: https://doi.org/10.1101/2021.01.22.21250282; this version posted February 6, 2021. The copyright holder for this preprint (which was not certified by peer review) is the author/funder, who has granted medRxiv a license to display the preprint in perpetuity. It is made available under a CC-BY 4.0 International license .

Table A.2.3c Parameters for the generation of secondary school contact networks.

Parameter	Value	Additional description
Number of grades	4	
Number of students per grade	200	
Number of teachers	125	
Number of staff	75	
Number of classes per student	6	Number of classes that each student takes each day; i.e., number of teachers with whom each student is connected
Percentage of student-teacher grade level matches	75%	Probability that a student takes a class with, i.e., connects to, a teacher that is associated with their own grade level
Number of student social groups per grade	20	FARZ parameter for student layers: Number of network clusters in each student layer
Student mean intra-grade degree	16	Average number of connections each student makes with students in the same grade
Student percent inter-grade contacts	20%	Percent of each student's total student connections that are with students in another grade
Number of teacher/staff groups	10	FARZ parameter for teacher/staff layers: Number of network clusters
Teacher/staff mean degree	10	Average number of connections each teacher/staff makes with other teachers/staff
`alpha`	5	FARZ parameter for all layers: Strength of common neighbor's effect on edge formation (tunes transitivity, clustering)
`gamma`	5	FARZ parameter for all layers: Strength of degree similarity effect on edge formation (tunes assortativity)
`beta`	0.8	FARZ parameter for all layers: Probability of edges formation within clusters (strength of cluster structure)
`r`	2	FARZ parameter for all layers: Maximum number of clusters each node can belong to
`q`	0.5	FARZ parameter for all layers: Probability of a node belonging to the multiple clusters

medRxiv preprint doi: https://doi.org/10.1101/2021.01.22.21250282; this version posted February 6, 2021. The copyright holder for this preprint (which was not certified by peer review) is the author/funder, who has granted medRxiv a license to display the preprint in perpetuity. It is made available under a CC-BY 4.0 International license .

Table A.2.3d Degree distribution plots for a representative secondary school network and network property statistics averaged across all primary school contact networks used in our analysis.

Network	Degree distribution	Network properties
Overall network	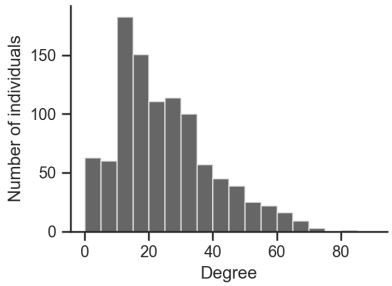	Degree mean: 24.1 Degree std: 15.0 Degree CV^2: = 0.39 Degree assortativity: -0.10 Clustering coeff.: 0.16 Average path length: 2.6
Student-Student layer	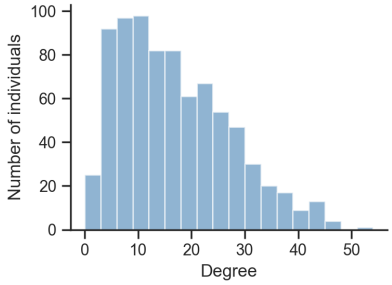	Degree mean: 16.0 Degree std 10.1 Degree CV^2 = 0.39 Degree assortativity: 0.16 Clustering coeff.: 0.22 Average path length: 2.9
Teacher-Staff layer	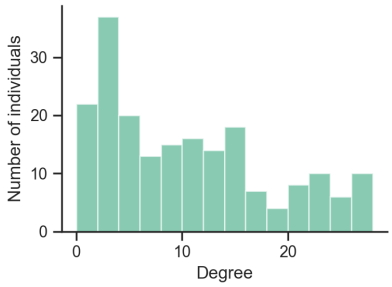	Degree mean 10.0 Degree std 8.2 Degree CV^2 = 0.64 Degree assortativity: 0.39 Clustering coeff.: 0.40 Average path length: 2.7

medRxiv preprint doi: https://doi.org/10.1101/2021.01.22.21250282; this version posted February 6, 2021. The copyright holder for this preprint (which was not certified by peer review) is the author/funder, who has granted medRxiv a license to display the preprint in perpetuity. It is made available under a CC-BY 4.0 International license .

A.2.4 Case Introductions

Exposure to the community is modeled by randomly introducing new cases to the school population according to a Poisson process with an average introduction rate that corresponds to the community prevalence. Each day of the simulation, the number of introductions is drawn from a Poisson distribution using the given introduction rate as the Poisson parameter λ. Then for each exposure that is to be introduced (if greater than zero), an individual is drawn randomly from the population with selection probabilities proportional to the relative susceptibility of each individual. If the selected individual(s) are susceptible, they become exposed (infected)—otherwise they have been previously infected and their state is left unchanged. This process is handled within the simulation loop adapted from the SEIRS+ Intervention Simulation Loop (Appendix A.2.5.1).

We consider monthly, weekly, and daily introduction rates, as well as single introduction scenarios. These rates roughly correspond to the community prevalences shown in **??**. These associations between the community prevalence and the rate of introduction to the school population are approximated using the following method. The expected number of new cases to be generated in the overall community is approximated using the equation for the change in the number of infected individuals from the classic SIR model

$$dI_c = \frac{\beta_c S_c I_c}{N_c} = \beta_c S_c \pi_c \,,$$

where dI_c gives the expected number of new infections in the community per day, N_c is the size of the community, β_c is the average community transmission rate, S_c is the number of susceptible individuals in the community, and $\pi_c = I_c/N_c$ is the community prevalence (the subscript c denotes a community value). Then the number of these new cases that will land in the school population is assumed to be proportional to the ratio of the size of the school population to the overall community population.

$$\text{expected school introduction rate} = \frac{\beta_c S_c I_c}{N_c} \frac{N}{N_c} \,.$$

When the numbers of current and prior cases in the community (I_c and R_c, respectively) are small relative to the size of the community (i.e., $S_c \approx N_c$; this estimation will tend to overestimate the school introduction rate when there is significant susceptible depletion in the community), this can be simplified to a reasonable approximation that does not depend on the size of the overall community

$$\begin{aligned}
\text{expected school introduction rate} &= \frac{\beta_c S_c I_c}{N_c} \frac{N}{N_c} \\
&= \frac{\beta_c (N_c - I_c - R_c) I_c}{N_c} \frac{N}{N_c} \\
&\approx \frac{\beta_c N_c I_c}{N_c} \frac{N}{N_c} \\
&= \frac{\beta_c I_c}{N_c} N \\
&= \beta_c \pi_c N \,.
\end{aligned}$$

Thus the expected rate of introductions to the school population approximately equal to the product of the community transmission rate β_c, the community prevalence π_c, and the size of the school population N. The community transmission rate is equal to the effective reproduction number R_{eff} for the community divided by the average

medRxiv preprint doi: https://doi.org/10.1101/2021.01.22.21250282; this version posted February 6, 2021. The copyright holder for this preprint (which was not certified by peer review) is the author/funder, who has granted medRxiv a license to display the preprint in perpetuity. It is made available under a CC-BY 4.0 International license .

infectious period of the disease. Given estimates for these values, the introduction rate can be estimated. This method was used to estimate introduction rates for primary schools (N=528) and secondary schools (N=1,000) for R_{eff} in the range (1.0, 2.0), a mean infectious period of 6.5 days, and a range of community prevalence values. The community prevalence ranges for each introduction rate listed in Table A.2.4 are those prevalences for which the expected number of new cases per day in the school population is approximately equal to the listed introduction rate (monthly, weekly, or daily) for some Reff in (1.0, 2.0) using this method and these parameters.

	Corresponding Community Prevalence	
Introduction rate (Poisson λ)	Primary school (528 individuals)	Secondary school (1000 individuals)
Monthly (λ = 1/30)	0.02 - 0.04%	0.01 - 0.02%
Weekly (λ = 1/7)	0.1 - 0.2%	0.05 - 0.1%
Daily (λ = 1)	0.5 - 1%	0.25 - 0.5%

For R_{eff} in the 1.0–2.0 range.

Table A.2.4 Introduction rates and community prevalences. Given community transmission in the range of R_{eff} = 1.0–2.0, this table relates the prevalence of disease in the community to the frequency at which new cases are introduced into a school. Details of how these ranges are estimated are provided in Appendix A.2.4.

A.2.5 Interventions

We model several interventions for mitigating the spread of SARS-CoV-2. The SEIRS+ framework provides code for a simulation loop that can implement several interventions, including testing, tracing, and isolation. We make use of a subset of the features in this simulation loop (with minor modification) to implement the mitigation strategies studied in this work.

A.2.5.1 Simulation loop

The simulation loop repeatedly calls a function that iterates the Gillespie dynamics of the Extended SEIR Network Model, which determines the next compartment transition (transmission event or disease progression) that will take place, advances the simulation time to the time of that event, and executes the state update. Every time the simulation time crosses an integer value (i.e., a new day is reached), the simulation loop interfaces with the model and its nodes, states, and parameters to implement various intervention procedures. If the Gillespie time to the next event is greater than a day, the simulation advances by a maximum time step that is a fraction of a day to ensure that intervention days are not skipped or irregularly timed. The simulation loop performs the following updates each iteration:

1. Advance the Gillespie compartment transition dynamics
2. If a new day has been reached, execute the following; else Return to (1):
   (a) Update active contact networks and parameters according to the weekend and cohorting schedule when applicable (see Appendix A.2.5.3 Cohorting and Appendix A.2.3.5 Cohort contact networks).

medRxiv preprint doi: https://doi.org/10.1101/2021.01.22.21250282; this version posted February 6, 2021. The copyright holder for this preprint (which was not certified by peer review) is the author/funder, who has granted medRxiv a license to display the preprint in perpetuity. It is made available under a CC-BY 4.0 International license .

(b) Introduce new community exposure cases (see Appendix A.2.4 Case Introductions).

(c) Isolate symptomatic individuals who are compliant with self-isolation upon symptom onset (see Appendix A.2.5.4 Isolation).

(d) If the current day is part of the testing cadence, test individuals who are eligible for testing when applicable (see Appendix A.2.5.2 Testing); else skip.

(e) Isolate individuals who have received a positive test result (following the test result lag time) and in some cases their classmates when applicable (see Appendix A.2.5.4 Isolation)

(f) Return to (1)

More details about these interventions are provided in the following sections.

A.2.5.2 Testing

We consider proactive testing that is executed according to one of several testing cadences (including no testing) shown in Table A.2.5. These cadences define which groups of individuals are tested and on which days of the week. On a designated testing day, all individuals who are eligible to be in the testing pool are tested. An individual is considered part of the testing pool when they:

- Are a member of one of the groups designated in the testing cadence
- Are not currently in isolation
- Have not already had a positive test result
- Have not already recovered from the disease
- Have not been vaccinated
- Are compliant with testing

We assume that 100% of teachers and staff are compliant with testing, but 25% of students are non-compliant and thus never get tested. Students are assigned a compliance status randomly according to this probability when the model is initialized.

We model realistic temporal test sensitivities consistent with PCR tests. We assume 0% sensitivity for individuals in the exposed (latent) state. We assume 75% sensitivity for individuals in the first 2 days of their pre-symptomatic period and 80% sensitivity for any pre-symptomatic days beyond that. Sensitivities for symptomatic

Proactive Testing Cadence	Mon	Tue	Wed	Thu	Fri	Sat	Sun
No Testing							
Teachers Weekly	🟢🟡						
Teachers Semiweekly	🟢🟡			🟢🟡			
Everyone Weekly	🟢🟡🔵						
Everyone Semiweekly	🟢🟡🔵			🟢🟡🔵			

🟢 Teachers 🟡 Staff 🔵 Students

Table A.2.5 School testing cadences. We explore the consequences of five testing cadences, from no testing to testing all members of the school community twice a week. Once-weekly testing takes place every Monday, and Semiweekly testing takes place on Mondays and Thursdays.

medRxiv preprint doi: https://doi.org/10.1101/2021.01.22.21250282; this version posted February 6, 2021. The copyright holder for this preprint (which was not certified by peer review) is the author/funder, who has granted medRxiv a license to display the preprint in perpetuity. It is made available under a CC-BY 4.0 International license .

and asymptomatic individuals alike follow the time course shown in Figure A2, which follows from Levine-Tiefenbrun et al (64). We assume there are no false positives.

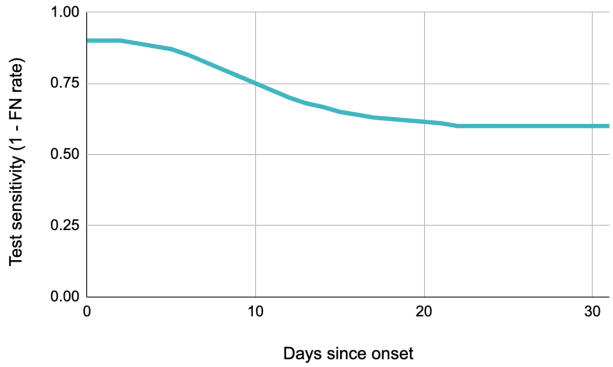

Figure A2: Test sensitivities. The probability of returning a positive test results when testing an individual in a symptomatic (I_{sym} or asymptomatic I_{asym} infectious state as a function of the number of days since entering that state (i.e., days since onset of symptoms). The test sensitivity is equivalent to 1 minus the false negative rate.

There is a 1 day lag (exactly 24 hours) between administering a test and receiving the result. Individuals that receive a positive result enter isolation (i.e., move into a quarantine compartment) immediately upon receiving the positive result, thus 1 day after being tested. We assume that all individuals in the school population are compliant with entering isolation upon a positive test result.

A.2.5.3 Cohorting

Cohorting consists of dividing students into two groups and following an alternating schedule in which only one group is on campus at a time. We consider two cohorting schedules, one where the group of students that is onsite alternates daily, and one where the onsite group alternates weekly (in addition to no cohorting). The cohorting schedules are summarized in Figure A3.

Cohort Schedule		Mon	Tue	Wed	Thu	Fri	Sat	Sun
All Students Onsite	Week 1	AB	AB	AB	AB	AB		
	Week 2	AB	AB	AB	AB	AB		
Alternate A/B Cohorts Daily	Week 1	A	B	A	B	A		
	Week 2	B	A	B	A	B		
Alternate A/B Cohorts Weekly	Week 1	A	A	A	A	A		
	Week 2	B	B	B	B	B		

A Cohort A on campus B Cohort B on campus

Figure A3

Cohorting is implemented by alternating between different versions of the contact network in which one group of students or the other has their connections with the school population removed, except for any connections to individuals in their own household. Global transmission remains active for students who are offsite due to the cohort schedule, which can be thought of as students having some propensity to interact with other members of the school population outside of school. We assume that all students comply with the cohorting schedule. Students

medRxiv preprint doi: https://doi.org/10.1101/2021.01.22.21250282; this version posted February 6, 2021. The copyright holder for this preprint (which was not certified by peer review) is the author/funder, who has granted medRxiv a license to display the preprint in perpetuity. It is made available under a CC-BY 4.0 International license .

who are offsite due to cohorting are not considered to be in isolation, and these students are still part of the testing pool when otherwise applicable.

A.2.5.4 Isolation

When an individual enters isolation, they are moved into the quarantine compartment that corresponds to their disease state at the time of isolation. This compartment transition is executed "manually" by the simulation loop, separate from the Gillespie or residence time-based transition dynamics (Appendix A.1.3 Dynamics). While in isolation, individuals transition between quarantine compartments according to the same disease state residence times that are used when not in isolation. The set of close contacts for isolated individuals is given by a distinct quarantine contact network, which includes connections to members of the quarantined individual's household but no other members of the school population. In addition, quarantined individuals make no casual contacts (i.e., no global transmission). Isolated individuals remain in the quarantine sequence of compartments until their total isolation period has elapsed, at which time they are moved into the non-quarantine compartment that corresponds to their current disease state. We use a 10 day isolation period for all individuals, following the current CDC recommendation (65).

In this model, individuals may enter isolation upon the onset of symptoms (if compliant), after receiving a positive test result, or when another member of their classroom has tested positive (for primary schools, when applicable).

We assume that 20% of all individuals elect to self-isolate upon the onset of symptoms. The symptomatic isolation compliance status of individuals is assigned randomly according to this probability when the model is initialized. For compliant individuals, there is a 1 day lag between transitioning into the symptomatic compartment and entering isolation. Individuals who are asymptomatic and thus enter the asymptomatic compartment rather

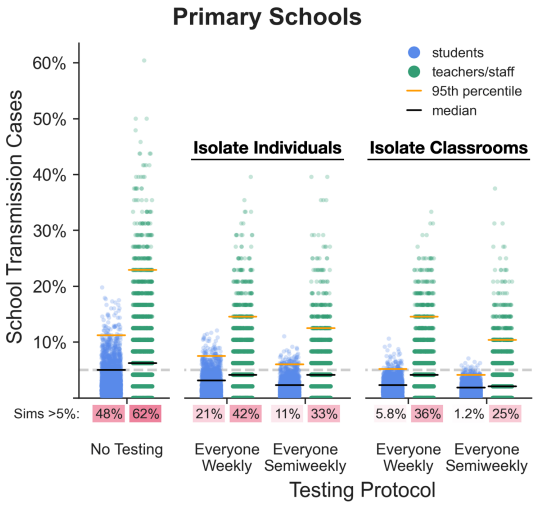

Figure A4: Effect of isolating classrooms. We consider two quarantine strategies for primary schools: (1) isolate single individuals who receive a positive test result, and (2) isolate the entire classroom (students and teacher) associated with an individual who receives a positive test. The distributions of school transmission cases as a percentage of the school population are shown for 1,000 simulations of each testing and isolation strategy with R_0=1.5 and approximately weekly new case introductions. Under each jitter distribution we list the percentage of simulations that result in outbreaks affecting more than 5% of the population. Black and orange lines represent median and 95th percentile outcomes respectively.

medRxiv preprint doi: https://doi.org/10.1101/2021.01.22.21250282; this version posted February 6, 2021. The copyright holder for this preprint (which was not certified by peer review) is the author/funder, who has granted medRxiv a license to display the preprint in perpetuity. It is made available under a CC-BY 4.0 International license .

than the symptomatic compartment never self-isolate. Note that the rate of asymptomatic disease is assumed to be different in primary school-aged children (40%) and adults/adolescents (30%) while the rate of symptomatic isolation compliance is constant, so the effective rate of symptomatic self-isolation is lower in young children.

In primary schools, where classroom groupings are stable, we also consider scenarios where entire classrooms (i.e., all students and the teacher) isolate when any one member of the classroom tests positive. In such a case, the entire group enters isolation at the same time immediately after the index case receives their test result (i.e., 1 day after being tested).

A.2.5.5 Vaccination

We also evaluate the effectiveness of vaccinating teachers and staff on mitigating transmission in schools. We use the following working definitions with regard to vaccination in this model:

- Uptake: The percentage of individuals who receive a vaccine
- Effectiveness: The percentage of individuals receiving the vaccine that have an efficacious response. An efficacious response is characterized by an immune response that protects the vaccinated individual from falling ill and that reduces the individual's transmissibility to some extent.
- Reduction in transmissibility: The factor by which individual transmissibility is reduced for individuals with an efficacious response to vaccination

We model the scenario where 100% of teachers and staff are vaccinated with a vaccine that has 90% effectiveness (and no students are vaccinated), and we consider scenarios where an effective vaccine blocks 100% of transmission (i.e., the vaccinated individual's transmissibility is reduced to 0) and where it only blocks 50% of transmission (i.e., the vaccinated individual's transmissibility is reduced to 50% its original value). The individuals that are to have an effective response are chosen randomly according to the probability of effectiveness when the model is initialized. Teachers are vaccinated and individuals with effective responses have their transmissibilities reduced before the simulation time begins. Individuals with effective immune responses are not included in case counts due to their immunity to the disease. Individuals with ineffective responses have no change in transmissibility or other parameters, can still contract and transmit the virus, and are included in case counts.